

Thermodynamic and energetic constraints on out-of-equilibrium tunneling rates

Ludovico Tesser,¹ Matteo Acciai,^{2,1} Christian Spånslätt,^{3,1} Inès Safi,⁴ and Janine Splettstoesser¹

¹*Department of Microtechnology and Nanoscience (MC2),
Chalmers University of Technology, S-412 96 Göteborg, Sweden*

²*Scuola Internazionale Superiore di Studi Avanzati, Via Bonomea 265, 34136, Trieste, Italy*

³*Department of Engineering and Physics, Karlstad University, Karlstad, Sweden*

⁴*Laboratoire de Physique des Solides (UMR 5802),*

CNRS-Université Paris-Sud and Paris-Saclay, Bâtiment 510, 91405 Orsay, France

(Dated: September 4, 2024)

We study bipartite quantum systems kept at different temperatures where a tunnel coupling between the two subsystems induces transitions. We find two independent constraints on the temperature-bias-dependent, out-of-equilibrium tunneling rates between the two subsystems, which both turn out to be particularly restrictive when the coupled quantum systems are small. These bounds take the form of a *thermodynamic* and of an *energetic* constraint, as they are associated with the dissipated heat and with the absorbed energy required to establish and deplete the temperature bias, respectively. The derived constraints apply to a large class of experimentally accessible quantum systems: except for the restriction to the tunneling regime, they hold for arbitrary subsystem Hamiltonians, including interactions or non-linear energy spectra. These results hold for a large class of experimentally relevant systems, ranging from molecular junctions to coupled cavities, and can be tested by, for instance, measuring the out-of-equilibrium tunneling current and its noise.

I. INTRODUCTION

Fluctuation theorems have been instrumental in studying the probability distribution of physical variables, such as thermodynamic work, in both classical and quantum stochastic thermodynamics [1–16]. In particular, detailed fluctuation theorems [7] constrain such probability distributions by relating the probability of a process to the probability of its time reverse. These relations provide a powerful framework to study fluctuations out of equilibrium, but they can also be used to, e.g., derive the equilibrium fluctuation-dissipation theorem (FDT) [17–19], which relates the fluctuations of observables to their dissipative responses. However, establishing a relation analogous to the FDT, linking generic correlations to response functions for systems *out of equilibrium* remains challenging [20–22]. For out-of-equilibrium correlated states, FDTs have been identified [23–27] for a generalized current operator, where its average and fluctuations are determined by two independent non-equilibrium transfer rates. Specifically, for a charge current induced by a voltage bias a FDT [28, 29] has been established far from equilibrium in the (*weak*) *tunneling regime*. In essence, this FDT extension relies on the detailed balance relation between these rates under the crucial assumption of a uniform temperature across the tunneling link. Consequently, the generalized FDT breaks down in the presence of a temperature bias.

However, setups with a temperature bias are crucial in (quantum) thermodynamics, where they are used to fuel, e.g., heat engines [30–32]. Pivotal experiments have not only implemented nanoscale heat engines [33–36] but also explored temperature biases for transport spectroscopy [37–40]. Importantly, systems exposed to large temperature biases also occur when one subsystem is cooled down with the help of coupling to an

other, possibly very different, subsystem [41–43]. Moreover, in nanoelectronics, systems with a temperature bias have attracted considerable attention in recent years in the context of so-called delta- T noise [44]. Several experiments [45–48] have detected this type of out-of-equilibrium charge noise generated by a temperature bias motivating further theoretical works [49–56]. These diverse efforts call for a better understanding of how a temperature bias constrains the dynamics of small-scale devices.

In particular, for nanoelectronics systems, fluctuation-dissipation bounds have recently been developed [57] for current fluctuations (or noise) in the presence of a temperature bias. While these bounds apply to conductors with generic transmission properties, their validity is limited to systems with weak electron-electron interactions. In the presence of possibly strong interactions, the perturbative approach developed in Refs. [24–27] showed that noise is super-Poissonian in the tunneling regime, even in the presence of a temperature bias. However, while the approach is general and not restricted to electronic systems, this constraint is rather loose and the role of the temperature bias is not singled out. Hence, there remains the important question of whether fundamental bounds on the noise or, more generally, on the tunneling dynamics exist also for strongly interacting systems accounting for the impact of a temperature bias.

In this work, we establish bounds on the nonequilibrium tunneling rates in the presence of a possibly large temperature bias accounting for the thermodynamic quantities required to generate such a temperature bias. To this end, we investigate the properties of the tunneling rates that characterize generic tunneling in a bipartite quantum system under arbitrary temperature biases. However, compared to earlier studies, we take a different approach in studying these out-of-equilibrium

rates: Instead of comparing the rate of a process, say Γ_{\rightarrow} , with the rate of its reversed process, Γ_{\leftarrow} , we compare the full out-of-equilibrium rates for subsystems at *different inverse temperatures*, $\Gamma_{\rightleftarrows}(\beta_L, \beta_R)$, with the rates of the same process but in the *absence of a temperature bias*: $\Gamma_{\rightleftarrows}(\beta_R, \beta_R)$. This approach allows us to prove two constraints on the tunneling rates which relate the cost of establishing a temperature bias to the response of the rates to a temperature change. These findings have direct implications on how the noise in systems subject to a temperature bias is constrained by the system dynamics. We thereby extend the scope of out-of-equilibrium noise at the intersection of quantum transport and quantum thermodynamics to systems with possibly strong interactions.

The main results of this paper are the thermodynamic constraint (Sec. III A) and the energetic constraint (Sec. III B) on the temperature-bias-dependent tunneling rates. These constraints connect the the out-of-equilibrium response of the tunneling rates to a temperature change to the thermodynamic and energetic costs of establishing a temperature bias, and take the form

$$\mathcal{W}^{(\text{Thermo})} \geq \mathcal{W}^{(\text{Resp})}, \quad (1a)$$

$$\mathcal{W}^{(\text{Energy})} \geq \mathcal{W}^{(\text{Resp})}. \quad (1b)$$

Here,

$$\mathcal{W}_{\rightleftarrows}^{(\text{Resp})} \equiv \partial_L \Gamma_{\rightleftarrows}(\beta_L, \beta_R) - \partial_L \Gamma_{\rightleftarrows}(\beta_R, \beta_R), \quad (2)$$

accounts for the response of $\Gamma_{\rightleftarrows}$ to a small change in the inverse temperature of the left (L) subsystem, both in the presence and in the absence of a temperature bias. Here, L is the subsystem that is taken at a different temperature when going from the configuration at a uniform temperature to that with a temperature bias. By contrast, $\mathcal{W}^{(\text{Thermo})}$ and $\mathcal{W}^{(\text{Energy})}$ are a thermodynamic and an energetic cost function, associated with the heat and with the energy required to change the temperature of subsystem L, respectively. More specifically, in the thermodynamic cost function

$$\mathcal{W}_{\rightleftarrows}^{(\text{Thermo})} \equiv \tilde{Q}^{(c)} \Gamma_{\rightleftarrows}(\beta_L, \beta_R) + \tilde{Q}^{(h)} \Gamma_{\rightleftarrows}(\beta_R, \beta_R), \quad (3)$$

the tunneling rates with and without the temperature bias are weighted by the minimal amount of heat, $\tilde{Q}^{(h/c)}$, dissipated to establish or to deplete the temperature bias of interest, $\beta_L - \beta_R$. In the energetic cost function,

$$\mathcal{W}_{\rightleftarrows}^{(\text{Energy})} \equiv \int_{U_L(\beta_R)}^{U_L(\beta_L)} \Gamma_{\rightleftarrows}(x, \beta_R) d[U_L(x)] \quad (4)$$

the tunneling rates are instead weighted by the amount of internal energy $dU_L(x)$ required for an infinitesimal increase of the temperature of subsystem L.

These general statements on the tunneling rates provide constraints also on the full out-of-equilibrium tunneling current noise, including the configuration with a temperature bias. This follows from a direct connection

between the tunneling rates and both average and fluctuations of the tunneling current flowing between the two parts of the bipartite system. Importantly, our findings do not rely on any close-to-equilibrium fluctuation theorems and our results hold for generic bipartite quantum systems, where strong correlations within each subsystem might be present.

The remainder of this paper is organized as follows. After a brief description of our generic theoretical model in Sec. II, we present constraints on out-of-equilibrium rates in Sec. III. In Sec. IV, we showcase the constraints for two experimentally relevant example systems. Several Appendices provide details of our derivations of key equations.

II. THEORETICAL MODEL

We study a bipartite system with Hamiltonian $\hat{H}_0 = \hat{H}_L + \hat{H}_R$, where subsystems L (left) and R (right) may be taken as generic systems, possibly with strong interactions. They are coupled to each other by the tunneling Hamiltonian

$$\hat{V}(t) = \hat{A} e^{-i\omega t} + \hat{A}^\dagger e^{i\omega t}, \quad (5)$$

which we assume to be a small perturbation, and which induces transitions in the subsystems. Further, in the weak tunnel-coupling regime, we describe the total system with the product state $\hat{\rho} = \hat{\tau}_L \otimes \hat{\tau}_R$, where $\hat{\tau}_\alpha \equiv \exp(-\beta_\alpha \hat{H}_\alpha)/Z_\alpha$ is the Gibbs state at inverse temperature β_α with partition function $Z_\alpha \equiv \text{Tr}_\alpha \{ \exp(-\beta_\alpha \hat{H}_\alpha) \}$. With this, we express the rates $\Gamma_{\rightleftarrows}$, induced by the coupling, to absorb or emit a quantum of energy $\hbar\omega$ in the spectral representation [17], as

$$\begin{aligned} \Gamma_{\rightarrow} &\equiv \frac{2\pi}{\hbar} \sum_{nmlk} |\mathcal{A}_{nmlk}|^2 \delta(\epsilon_{mn}^{(L)} + \epsilon_{kl}^{(R)} - \hbar\omega) p_n^{(L)} p_l^{(R)}, \\ \Gamma_{\leftarrow} &\equiv \frac{2\pi}{\hbar} \sum_{nmlk} |\mathcal{A}_{nmlk}|^2 \delta(\epsilon_{mn}^{(L)} + \epsilon_{kl}^{(R)} - \hbar\omega) p_m^{(L)} p_k^{(R)}, \end{aligned} \quad (6)$$

with their dependence on ω and inverse temperatures β_α left implicit. Here, $\mathcal{A}_{nmlk} \equiv \langle mk | \hat{A} | nl \rangle$ is the matrix element of \hat{A} in the basis of the eigenstates of the generic Hamiltonian \hat{H}_0 , namely $\hat{H}_L |nl\rangle = \epsilon_n^{(L)} |nl\rangle$, and $\hat{H}_R |nl\rangle = \epsilon_l^{(R)} |nl\rangle$. Furthermore, we have defined the energy differences $\epsilon_{mn}^{(\alpha)} \equiv \epsilon_m^{(\alpha)} - \epsilon_n^{(\alpha)}$, and the occupation probability of the state $|n\rangle$ as $p_n^{(\alpha)} |n\rangle = \hat{\tau}_\alpha |n\rangle$. Note that the partition of the system into two subsystems is not required to derive Eq. (6) (see Appendices A, B and references therein) but is needed to implement a well-defined temperature bias. The scope of the present paper is to find bounds for these rates in the presence of such a temperature bias. It is therefore important to point out here that the temperature dependence of the tunneling rates enters only through the occupation probabilities $p_n^{(\alpha)}$.

The two tunneling rates in Eq. (6) are the key quantities that determine the transitions between subsystems L and R. To show this connection, we consider an observable, represented by the operator \hat{Q} that commutes with \hat{H}_0 , i.e. $[\hat{Q}, \hat{H}_0] = 0$, but does not commute with the tunneling Hamiltonian $\hat{V}(t)$. For simplicity, we here focus on operators satisfying $[\hat{Q}, \hat{A}] = q\hat{A}$, meaning that the transitions induced by the operator \hat{A} transfer exactly one quantum q . Nonetheless, more general results that do not rely on this assumption are provided in Appendix B. The rate of change of the observable \hat{Q} defines the current operator

$$\hat{I}(t) = -\frac{iq}{\hbar} \left(\hat{A}e^{-i\omega t} - \hat{A}^\dagger e^{i\omega t} \right). \quad (7)$$

By treating the tunneling Hamiltonian $\hat{V}(t)$ perturbatively, we study the average current $I = I(t) \equiv \langle \hat{I}_H(t) \rangle$ and its zero frequency noise $\mathcal{S} \equiv \int dt \langle \delta \hat{I}_H(t) \delta \hat{I}_H(0) \rangle$, where $\hat{I}_H(t)$ is the current operator in the Heisenberg picture and $\delta \hat{I}_H(t) \equiv \hat{I}_H(t) - I(t)$ its fluctuation.

In terms of the rates (6), the transport quantities I and \mathcal{S} , to lowest order in the perturbation, read [17, 24, 26]

$$\frac{I}{q} = \Gamma_{\rightarrow} - \Gamma_{\leftarrow}, \quad (8a)$$

$$\frac{\mathcal{S}}{q^2} = \Gamma_{\rightarrow} + \Gamma_{\leftarrow}, \quad (8b)$$

see also the derivation in Appendix A. Equation (8) shows that the tunneling current I counts the difference between single tunneling events in the two directions, weighted by the transferred quantum q . In contrast, the noise, being the variance of the transmitted charge, adds such events. This structure (difference/sum of tunneling rates) was shown to extend further to all odd/even higher-order cumulants [29]. From Eq. (8), one sees that the current noise is super-Poissonian, i.e. $\mathcal{S} \geq q|I|$, which holds true even for more general out-of-equilibrium distributions [24].

In the special—but most frequently studied—case when the two subsystems have the same inverse temperature $\beta_L = \beta_R \equiv \beta$, the occupation probabilities in Eq. (6) read

$$p_n^{(L)} p_l^{(R)} = \frac{\exp[-\beta(\epsilon_n^{(L)} + \epsilon_l^{(R)})]}{Z_L Z_R}. \quad (9)$$

This simplifies the rates in Eq. (6) significantly and implies the basic detailed balance relation $\Gamma_{\rightarrow}/\Gamma_{\leftarrow} = \exp(\beta\hbar\omega)$. Applying this simple relation to the current and its zero-frequency noise given in Eq. (8) leads to the out-of-equilibrium FDT [24, 26, 29]

$$\mathcal{S} = qI \coth\left(\frac{\beta\hbar\omega}{2}\right). \quad (10)$$

It relates the tunneling current I to the tunneling current noise \mathcal{S} , the tunneling charge q , the tunneling frequency

ω and the inverse temperature β . Only in the strict limit $\omega \rightarrow 0$, together with the condition $\beta_L = \beta_R$, the rates in Eq. (6) are equilibrium quantities and hence Eq. (10) reduces to the Nyquist-Johnson relation [58, 59]. However, when $\beta_L \neq \beta_R$, the relation (10) does not hold any longer [24, 57], and the *out-of-equilibrium* noise can have more intricate features. In the following, we focus on this temperature-biased setup and show how these features are limited by thermodynamic and energetic constraints on the tunneling rates and, as a consequence, on the tunneling current and its noise.

III. CONSTRAINTS ON OUT-OF-EQUILIBRIUM TUNNELING RATES

To highlight the critical role played by a sizable temperature difference, we spell out, in this Section and below, the temperature arguments explicitly. To this end, we denote by $\Gamma_{\rightarrow}(\beta_L, \beta_R)$ and $\Gamma_{\leftarrow}(\beta_L, \beta_R)$ the forward and backward out-of-equilibrium tunneling rates, where the first argument denotes the temperature subsystem L and the second the temperature of subsystem R. Without loss of generality, we also assume that, out of equilibrium, subsystem L is always hotter than subsystem R, i.e. $\beta_R > \beta_L$. We now compare the tunneling rates in the situation where the two subsystems have the same temperature, i.e., $\Gamma_{\rightleftarrows}(\beta_R, \beta_R)$, with those under the desired out-of-equilibrium condition, i.e., $\Gamma_{\rightleftarrows}(\beta_L, \beta_R)$. In what follows, for conciseness, we refer to the equal-temperature tunneling rates $\Gamma_{\rightleftarrows}(\beta_R, \beta_R)$ as *equilibrium* tunneling rates, even though we want to emphasize here that the dependence on the energy-transfer ω , see Eq. (6), implies the full treatment of possible nonequilibrium conditions beyond a temperature bias, induced by an external agent. Differently from detailed-balance relations or fluctuation theorems relating backward and forward processes to each other but at a given nonequilibrium situation or protocol [7, 15], we here compare forward to forward and backward to backward rates, however at different nonequilibrium conditions. We show that these tunneling rates, which are *transport* quantities, are related to each other via inequalities that also contain *thermodynamic* quantities like the internal energy $U_\alpha(\beta)$ and the entropy $S_\alpha(\beta)$ for $\alpha = L, R$. These are defined as

$$U_\alpha(\beta) \equiv \text{Tr}_\alpha \left\{ \hat{H}_\alpha \frac{e^{-\beta\hat{H}_\alpha}}{Z_\alpha(\beta)} \right\}, \quad (11)$$

$$S_\alpha(\beta) \equiv -\text{Tr}_\alpha \left\{ \frac{e^{-\beta\hat{H}_\alpha}}{Z_\alpha(\beta)} \log \frac{e^{-\beta\hat{H}_\alpha}}{Z_\alpha(\beta)} \right\}. \quad (12)$$

Below, we present two constraints on the tunneling rates: a thermodynamic and an energetic one. We further discuss how these constraints are relevant for small-scale systems which do not approach the thermodynamic limit.

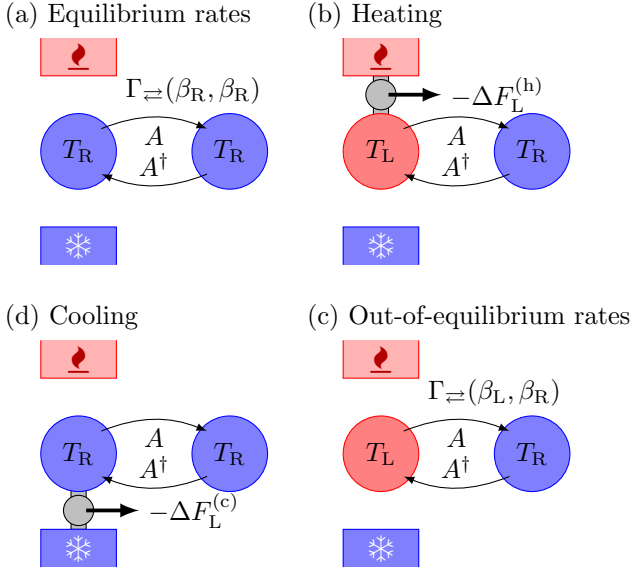


Figure 1. Thermodynamic cycle of a fictitious tunneling experiment. (a) The two subsystems have the same (cold) temperature $T_R = \beta_R^{-1}$, and tunneling events are described by the equilibrium rates $\Gamma_{\leftrightarrow}(\beta_R, \beta_R)$. (b) The left-hand (L) side is put into contact with a hot bath and heats up. In this process, the extracted work is at most $-\Delta F_L^{(h)}$ [Eq. (13)]. (c) The subsystems have now different temperatures, and tunneling events are described by the out-of-equilibrium rates $\Gamma_{\leftrightarrow}(\beta_L, \beta_R)$. (d) The system is brought back to the initial condition by putting the L side in contact with a cold bath. In this cooling process, the extracted work is at most $-\Delta F_L^{(c)}$ [Eq. (14)].

A. Thermodynamic constraint

To introduce the thermodynamic constraint, we consider the thermodynamic cycle in Fig. 1 that a *fictitious* experiment could undergo. The setup consists of the two subsystems L and R, between which the tunneling transitions occur, and two macroscopic baths fixed at the inverse temperatures β_L, β_R . These baths are used to change the temperature of the L subsystem. Initially, the fictitious experiment is prepared with the subsystems in equilibrium at the same cold temperature $T_R = \beta_R^{-1}$. Then, the following protocol is imagined to be carried out:

- (a) *Equilibrium rates*: Tunneling events occur between L and R, according to the rates $\Gamma_{\leftrightarrow}(\beta_R, \beta_R)$, i.e., in the situation where both subsystems are at the cold temperature T_R .
- (b) *Heating*: The hot bath at temperature $T_L = \beta_L^{-1}$ is brought into contact with subsystem L. Then, heat flows from the bath into subsystem L until the latter is heated up to T_L . This process induces a change in subsystem L's internal energy, given as $U_L(\beta_L) - U_L(\beta_R) \equiv \Delta U_L$ and of its entropy $S_L(\beta_L) - S_L(\beta_R) \equiv \Delta S_L$. Here, U_L and S_L

are given in Eqs. (11) and (12), respectively. While heat flows, one may extract work, which is at most $-\Delta F_L^{(h)}$ (see Appendix C for additional details), where

$$\Delta F_L^{(h)} \equiv \Delta U_L - T_L \Delta S_L, \quad (13)$$

is the nonequilibrium free energy change. After the heating process, we have reached the out-of-equilibrium condition of interest, where the two subsystems have different temperatures.

- (c) *Out-of-equilibrium rates*: The cold bath is now disconnected from subsystem L, and tunneling occurs between the subsystems at the out-of-equilibrium tunneling rates $\Gamma_{\leftrightarrow}(\beta_L, \beta_R)$.
- (d) *Cooling*: In this step, the total system is returned to the initial condition. This is done by bringing the cold bath at temperature T_R in contact with subsystem L. Then, heat flows out of subsystem L until it reaches temperature T_R , thus inducing the change $-\Delta U_L$ and $-\Delta S_L$ in internal energy and entropy, respectively. Similarly to the heating step (b), while heat is flowing it is possible to extract work, which is at most $-\Delta F_L^{(c)}$, where

$$\Delta F_L^{(c)} \equiv -\Delta U_L + T_R \Delta S_L \quad (14)$$

is the nonequilibrium free energy change.

With the quantities encountered during the cycle (a)-(d), we next define the thermodynamic cost function

$$\mathcal{W}_{\leftrightarrow}^{(\text{Thermo})} \equiv -\Delta F_L^{(c)} \eta^{(h)} \Gamma_{\leftrightarrow}(\beta_L, \beta_R) + -\Delta F_L^{(h)} \eta^{(c)} \Gamma_{\leftrightarrow}(\beta_R, \beta_R), \quad (15)$$

where $\Delta F_L^{(h,c)}$ is given in Eqs. (13, 14) and $\eta^{(c)} \equiv \frac{\beta_L}{\beta_R - \beta_L} = \frac{T_R}{T_L - T_R}$ and $\eta^{(h)} \equiv \frac{\beta_R}{\beta_R - \beta_L} = \frac{T_L}{T_L - T_R}$ correspond to the coefficient of performance of a refrigerator and of a heat pump, respectively. Crucially, the product $-\Delta F_L^{(h)} \eta^{(c)} \equiv \tilde{Q}^{(h)}$ sets a lower limit on the heat absorbed by the cold L subsystem during the heating process when the extracted work is maximum, as detailed in Appendix C. Similarly, the product $-\Delta F_L^{(c)} \eta^{(h)} \equiv \tilde{Q}^{(c)}$ sets a lower limit on the heat absorbed by the cold bath during the cooling process. Thus, in the thermodynamic cost function (15), the equilibrium and out-of-equilibrium tunneling rates Γ_{\leftrightarrow} are weighted by the heat dissipated to reach the opposite, namely out-of-equilibrium and equilibrium, conditions.

The thermodynamic cost function satisfies the following inequality (see Appendix D for the derivation)

$$\mathcal{W}_{\leftrightarrow}^{(\text{Thermo})} \geq \mathcal{W}_{\leftrightarrow}^{(\text{Resp})}, \quad (16)$$

where the rate response $\mathcal{W}_{\leftrightarrow}^{(\text{Resp})}$ is defined as

$$\mathcal{W}_{\leftrightarrow}^{(\text{Resp})} \equiv \partial_L \Gamma_{\leftrightarrow}(\beta_L, \beta_R) - \partial_L \Gamma_{\leftrightarrow}(\beta_R, \beta_R), \quad (17)$$

and $\partial_L \Gamma_{\rightleftarrows}(x, y) \equiv \frac{\partial \Gamma_{\rightleftarrows}}{\partial x}(x, y)$ is the derivative with respect to the first argument of $\Gamma_{\rightleftarrows}(x, y)$. The rate response $\mathcal{W}_{\rightleftarrows}^{(\text{Resp})}$ accounts for both the equilibrium and out-of-equilibrium response of the tunneling rates to a change in the temperature of subsystem L. Equation (16) is the first central result of this work. It implies that the response of the (nonequilibrium) rates to a change in temperature is limited by the rates themselves and by the thermodynamic cost for setting the temperature bias.

We emphasize that Eq. (16) directly translates into a constraint on the out-of-equilibrium noise, which is given by the sum of the tunneling rates via Eq. (8b). This also means, from a more practical, experimental viewpoint, that one possibility to test the constraint (16) is by measuring the noise and tunneling current in two configurations: (i) When both subsystems have the same cold temperature, and (ii) in the desired out-of-equilibrium condition. One can then access the tunneling rates as $2q^2 \Gamma_{\rightleftarrows} = \mathcal{S} \pm qI$. All the other quantities entering the inequality can be calculated once the state of the subsystem considered at the different temperatures is known [60].

From the thermodynamic constraint (16), we can derive a direct lower bound on the out-of-equilibrium tunneling rates $\Gamma_{\rightleftarrows}(\beta_L, \beta_R)$ in terms of the equilibrium rates (see the derivation in Appendix E). These constraints furthermore contain the rate response, (integrals of) thermodynamic quantities and it reads

$$\begin{aligned} \Gamma_{\rightleftarrows}(\beta_L, \beta_R) \geq \Gamma_{\rightleftarrows}(\beta_R, \beta_R) \exp \left[\int_{\beta_L}^{\beta_R} g(x) dx \right] + \\ - \int_{\beta_L}^{\beta_R} f(x) \exp \left[\int_{\beta_L}^x g(s) ds \right] dx, \end{aligned} \quad (18)$$

where we define

$$\begin{aligned} f(x) &\equiv \partial_L \Gamma_{\rightleftarrows}(\beta_R, \beta_R) - \Delta F_L^{(\text{c})}(x) \eta^{(\text{h})}(x) \Gamma_{\rightleftarrows}(\beta_R, \beta_R), \\ g(x) &\equiv -\Delta F_L^{(\text{h})}(x) \eta^{(\text{c})}(x). \end{aligned} \quad (19)$$

While the bound (18) has a more complex shape, containing integrals over thermodynamic functions, it has the important advantage that it does not depend on the out-of-equilibrium responses $\partial_L \Gamma_{\rightleftarrows}(\beta_L, \beta_R)$. Instead, only the more easily accessible *equilibrium response function*, $\partial_L \Gamma_{\rightleftarrows}(\beta_R, \beta_R)$, enters Eq. (18). We emphasize that Eq. (18) directly provides a lower bound for the out-of-equilibrium noise. In particular, compared to [24], it provides a nontrivial constraint on *how much* super-Poissonian the noise is.

B. Energetic constraint

In this subsection, we show that the rate response functions, $\mathcal{W}_{\rightleftarrows}^{(\text{Resp})}$ in Eq. (17), impose another constraint on the rates $\Gamma_{\rightleftarrows}$ themselves, which, unlike the thermodynamic constraint of Eq. (16), does not focus on the thermodynamic cost required to generate the temperature

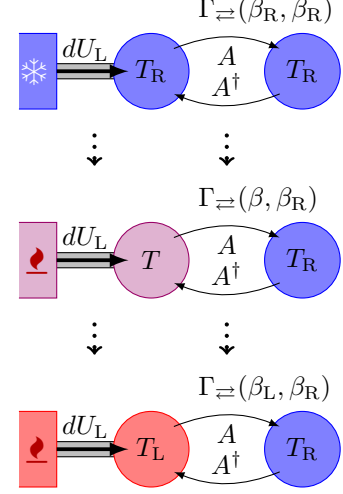


Figure 2. Heating stroke of the left (L) subsystem. As the temperature of L increases from T_R to T_L (top to bottom panels), the energy absorbed, dU_L , and the tunneling rates, $\Gamma_{\rightleftarrows}(\beta, \beta_R)$, are monitored at each intermediate temperature.

bias, but rather on the energetic cost. Therefore, this second constraint does not require considering the whole cycle (a)-(d), but only the heating stroke (d).

Starting from subsystem L being at the cold temperature $T_R = \beta_R^{-1}$, we imagine slowly increasing its temperature and identifying the tunneling rates at each temperature. This procedure is depicted in Fig. 2. Next, by weighting the tunneling rates with the corresponding variation of the internal energy needed to increase the temperature of subsystem L, we identify the following energetic cost function $\mathcal{W}_{\rightleftarrows}^{(\text{Energy})}$ and the corresponding constraint (see Appendix F for the derivation)

$$\mathcal{W}_{\rightleftarrows}^{(\text{Energy})} \equiv \int_{U_L(\beta_R)}^{U_L(\beta_L)} \Gamma_{\rightleftarrows}(x, \beta_R) d[U_L(x)] \geq \mathcal{W}_{\rightleftarrows}^{(\text{Resp})}. \quad (20)$$

Equation (20) is the second central result of this work. In contrast to the thermodynamic constraint (16), Eq. (20) involves only the internal energy of subsystem L, i.e., $U_L(\beta)$. This difference between Eq. (16) and Eq. (20) is also reflected on the conditions required to saturate the two constraints. By construction, both thermodynamic and energetic bounds become equalities in the zero temperature-bias regime, $\beta_L = \beta_R$. However, in this regime Eqs. (16, 20) become trivial since $\mathcal{W}^{(\text{Thermo})} = \mathcal{W}^{(\text{Energy})} = \mathcal{W}^{(\text{Resp})} = 0$. Nonetheless, the constraints can be saturated non-trivially in the presence of a temperature bias when the tunneling transitions involve states of subsystem L with a specific energy, only. While for the thermodynamic constraint this energy corresponds to the energy at which the Gibbs distribution at different temperatures cross $p_n^{(L)}(\beta_L) = p_n^{(L)}(\beta_R)$ (see Appendix D), for the energetic constraint this energy is the internal energy of the L subsystem U_L (see Appendix F).

Similarly to the thermodynamic constraint, Eq. (20)

directly translates into an energetic constraint on the integral over the out-of-equilibrium noise in Eq. (8b) by taking the sum of the energetic constraints for both tunneling directions. However, this integral makes the energetic constraint less relevant from an experimental point of view because it requires knowledge of both internal energy and tunneling rates at all intermediate temperatures of subsystem L.

Note that the derivations of both thermodynamic and energetic constraints do in principle not require the temperatures of the two subsystems to be equal neither at the beginning nor at end of any of the strokes (see Appendix D and F). Here, however, we choose one of the settings where the two subsystems have equal temperature, in order to be able to compare to an easily accessible, experimentally relevant reference situation when establishing the out-of-equilibrium tunneling-rate constraints.

C. Thermodynamic limit

Here, we comment on the relevance of the discovered constraints (16) and (20) for subsystems that approach the thermodynamic limit. Notably, both the thermodynamic and the energetic constraints combine *transport* quantities, i.e., the tunneling rates, with *extensive* properties of subsystem L, namely its internal energy and its nonequilibrium free energy. However, the extensive quantities only appear on the left-hand side of Eqs. (16, 20), and not on the right-hand side. This feature implies that the left- and the right-hand sides behave very differently depending on the size of the system. More concretely, if the extensive quantities in the thermodynamic limit scale as

$$U_L \rightarrow \lambda U_L, \quad \Delta F_L^{(c,h)} \rightarrow \lambda \Delta F_L^{(c,h)}, \quad (21)$$

where λ is the scale parameter, and the tunneling rates scale with an arbitrary scaling function $f(\lambda)$, i.e. $\Gamma_{\rightleftarrows} \rightarrow f(\lambda) \Gamma_{\rightleftarrows}$, both the thermodynamic constraint of Eq. (16) and the energetic constraint of Eq. (20) become trivial. Indeed, for $\lambda \rightarrow \infty$, the right-hand side containing the rate response $\mathcal{W}_{\rightleftarrows}^{(\text{Resp})}$ becomes negligible, and Eqs. (16, 20) then reduce to expressions that state the positivity of the thermodynamic and energetic costs, respectively, on the left-hand side. For instance, we can imagine replacing subsystem L with λ copies of it, but take only one of the copies to be connected to subsystem R through the tunneling Hamiltonian $\hat{V}(t)$. Then, the internal energy and the entropy of the λ copies are given as $U_{\lambda L}(\beta) = \lambda U_L(\beta)$ and $S_{\lambda L}(\beta) = \lambda S_L(\beta)$, respectively. This linear scaling implies that also the nonequilibrium free energy scales linearly with λ , i.e., $\Delta F_{\lambda L}^{(c,h)} = \lambda \Delta F_L^{(c,h)}$. By stark contrast, both the temperatures T_L , T_R and the tunneling rates remain unchanged because the former are intensive properties and the latter are transport properties that involve only one of the copies. Therefore, in the thermodynamic limit, the left-hand sides of both thermodynamic

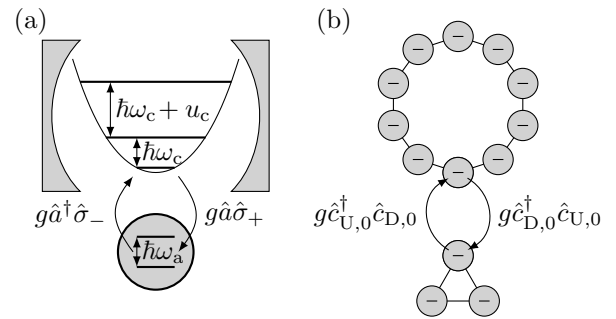


Figure 3. Illustration of the two setups considered in Sec. IV. (a) A two-level atom with frequency ω_a is weakly coupled, $g \ll \hbar\omega_{a,c}$, to a cavity with characteristic frequency ω_c and Kerr non-linearity u_c . (b) Two interacting fermionic tight-binding rings with different sizes are weakly coupled at a single (“0”) site.

and energetic constraints of Eqs. (16, 20) scale with λ whereas the right-hand sides do not.

However, the fact that the right hand sides of these equations can be neglected in the thermodynamic limit—*independently* on how it is taken—leads to a trivial statement. The thermodynamic and energetic costs are positive by construction: The tunneling rates are positive $\Gamma_{\rightleftarrows} \geq 0$, and so are the coefficients of performance $\eta^{(c,h)} \geq 0$, the nonequilibrium free energies $-\Delta F_L^{(c,h)} \geq 0$, as well as the energy variation $dU_L(x)$ in the integral in Eq. (20).

Thus, for both the thermodynamic and the energetic constraint to be insightful, subsystem L (namely the subsystem which we consider at two different temperatures in order to compare tunneling rates) must be a small quantum system, namely it must *not* satisfy the thermodynamic limit.

IV. EXAMPLES

To illustrate the constraints derived in Sec. III, we consider two different physical settings, represented by the systems depicted in Fig. 3: An atom coupled to a nonlinear cavity [panel (a)], and two fermionic chains interchanging particles at a single site [panel (b)]. Such examples are chosen not only because of illustration purposes, but also because they are of experimental relevance to test our predictions with state-of-the art setups. These two examples include optical or mechanical cavities coupled together [61] or to (artificial) atoms [62–67], and tunneling bridges across molecules [38, 40, 68] or magnetic impurities [69–71].

To clarify the constraints of Eqs. (16, 20), we notice that both the thermodynamic, $\mathcal{W}_{\rightleftarrows}^{(\text{Thermo})}$, and energetic cost, $\mathcal{W}_{\rightleftarrows}^{(\text{Energy})}$, as well as the rate response $\mathcal{W}_{\rightleftarrows}^{(\text{Resp})}$ entering the constraints can be recast as sums over reso-

nances as

$$\mathcal{W}_{\pm}^{(i)} = \sum_{nmlk} w_{\pm,nmlk}^{(i)} \delta(\epsilon_{mn}^{(\text{L})} + \epsilon_{kl}^{(\text{R})} - \hbar\omega), \quad (22)$$

where $i \in \{\text{Thermo, Energy, Resp}\}$. This is done by using the expression of the rates in Eq. (6) and the definitions in Eqs. (15, 17, 20). In the following, we focus on the amplitude of the resonance ω of interest by considering

$$\mathcal{C}_{\leftrightarrow}^{(i)}(\omega) \equiv \sum_{\{nmlk | \epsilon_{mn}^{(\text{L})} + \epsilon_{kl}^{(\text{R})} = \hbar\omega\}} w_{\leftrightarrow,nmlk}^{(i)}, \quad (23)$$

and thus sum over all the resonances at the same frequency ω . Since both the thermodynamic and energetic constraints hold separately at each resonance, Eqs. (16, 20) also hold for each amplitude $\mathcal{C}_{\leftrightarrow}^{(i)}(\omega)$, i.e.

$$\begin{aligned} \mathcal{C}_{\leftrightarrow}^{(\text{Thermo})}(\omega) &\geq \mathcal{C}_{\leftrightarrow}^{(\text{Resp})}(\omega), \\ \mathcal{C}_{\leftrightarrow}^{(\text{Energy})}(\omega) &\geq \mathcal{C}_{\leftrightarrow}^{(\text{Resp})}(\omega), \end{aligned} \quad (24)$$

which establishes natural quantities to compute in our analysis of the systems depicted in Fig. 3.

A. Atom coupled to nonlinear cavity

In this section, we consider an atom weakly coupled to a nonlinear cavity [72]. Its Hamiltonian is given by

$$\hat{H} = \hbar\omega_a \frac{\hat{\sigma}_z}{2} + \hbar\omega_c \hat{n} + \frac{u_c}{2} \hat{n}(\hat{n} - 1) + g(\hat{a}\hat{\sigma}_+ + \hat{a}^\dagger\hat{\sigma}_-). \quad (25)$$

Here, one of the subsystems is the atom, described by the Pauli matrix $\hat{\sigma}_z$ and has the atom frequency ω_a . The cavity is the other subsystem, and is described by the number operator $\hat{n} = \hat{a}^\dagger\hat{a}$, with $[\hat{a}, \hat{a}^\dagger] = 1$, and the cavity frequency ω_c . We also include a Kerr nonlinearity, parametrized by u_c , which plays the role of effective interactions between cavity photons in this system. The atom and the cavity exchange photon quanta through the weak tunneling term $g(\hat{a}\hat{\sigma}_+ + \hat{a}^\dagger\hat{\sigma}_-)$ with $g \ll \hbar\omega_{a,c}$ and where $\hat{\sigma}_+$ and $\hat{\sigma}_-$ are the raising and lowering operators of the atom states. Note that we choose $\omega = 0$ since any external driving frequency can be incorporated in the laser detuning—replacing ω_c —in the rotating frame [42]. For $u_c = 0$, the Hamiltonian (25) reduces to the Jaynes-Cummings Hamiltonian [73].

To relate to the theoretical framework of Sec. II, we now identify the tunneling operator $\hat{A} = g\hat{a}\hat{\sigma}_+$, which we use to calculate the zero-frequency amplitudes $\mathcal{C}_{\leftrightarrow}^{(i)}(0)$ in Eq. (23). Note that a possible observable \hat{Q} could here be the atomic occupation $\hat{Q} = \frac{\hat{\sigma}_z+1}{2}$, satisfying $[\hat{Q}, \hat{A}] = \hat{A}$. The result for $\mathcal{C}_{\leftrightarrow}^{(i)}(0)$ is shown in Fig. 4, where we plot $\mathcal{C}_{\leftrightarrow}^{(i)}(0)$ for different values of the non-linearity u_c . Since we are free to choose the L subsystem, in panels (a, c) the

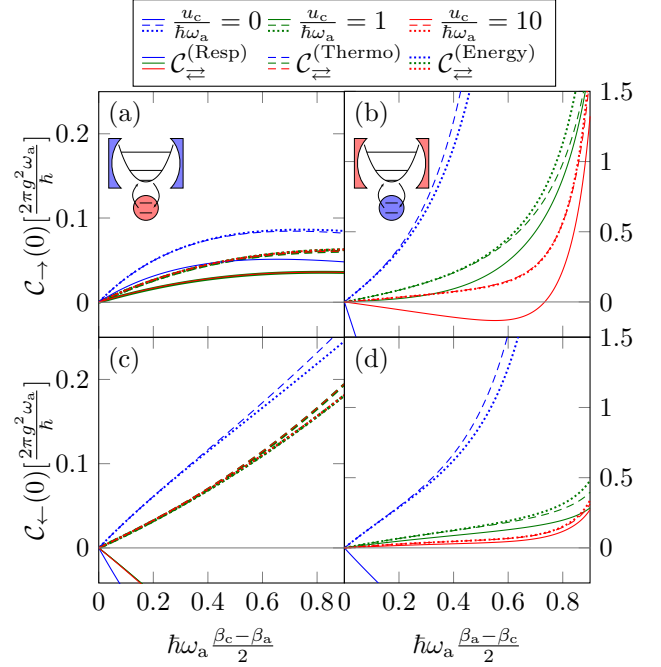


Figure 4. Thermodynamic cost (dashed lines), energetic cost (dotted lines), and rate response (solid lines) for an atom coupled to a cavity as functions of the inverse temperature difference $\beta_a - \beta_c$. The atom and cavity frequencies are taken in resonance, $\omega_a = \omega_c$, and the different curve colors denote different Kerr nonlinearities, $u_c/\hbar\omega_a = 0, 1, 10$, in blue, green, and red, respectively. In panels (a, c) the cavity is kept at the cold temperature ($\beta_c > \beta_a$), whereas in panels (b, d) it is the atom that has the colder temperature ($\beta_a > \beta_c$).

atom is the subsystem considered at two different temperatures, whereas in panels (b, d) the cavity is. Here we see that both thermodynamic and energetic constraints are trivially saturated at equal temperature. However, for sizable temperature biases, considering the atom or the cavity at different temperatures affects the constraints. In particular, in panels (b, d) we see that the cavity non-linearity allows to approach both thermodynamic and energetic constraints also at large temperature biases for both rates Γ_{\leftrightarrow} . The non-linearity affects the constraints (24) in two ways: On the one hand, finite values of u_c break the degeneracy of the atom-cavity transitions, making the atom couple only to two consecutive cavity states. On the other hand, a large u_c increases the energy spacing of the cavity. This feature reduces the number of states that have non-negligible occupation at finite cavity temperature $\beta_c \neq 0$. These two aspects effectively reduce the dimension of the cavity, moving it further away from the thermodynamic limit.

By contrast, when it is instead the atom that is taken at two different temperatures, illustrated in panels (a, c), the rate Γ_{\rightarrow} has a nontrivial constraint for all temperature biases, while the rate Γ_{\leftarrow} does not. This stems from the transitions allowed by the tunneling operator \hat{A} in the reverse process, which here consists of only the

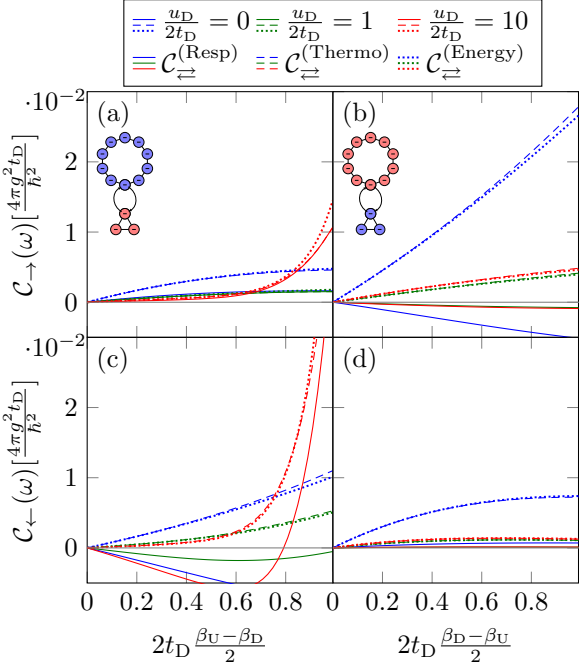


Figure 5. Thermodynamic cost (dashed lines), energetic cost (dotted lines), and rate response (solid lines) for two (U and D) coupled fermionic rings with sizes $L_D = 3$ and $L_U = 10$. The costs are plotted vs the inverse temperature difference $\beta_D - \beta_U$. The ring hopping parameters, t_D and t_U , and the driving frequency are fixed as $t_U = \frac{4}{5}t_D = 2\hbar\omega$. The upper ring charging energy $u_U = 0$ is also fixed, while the down ring charging energy is taken as $u_D/2t_D = 0, 1, 10$ for curves in blue, green, and red, respectively. In panels (a, c) the upper, larger ring is kept at the cold temperature ($\beta_U > \beta_D$), whereas in panels (b, d) it instead is the down, smaller ring that is colder ($\beta_L > \beta_U$).

process in which the atom emits a photon into the cavity, combined with the energy spectrum of such allowed transitions. Specifically, if all allowed transitions start in states with energies that are more than a standard deviation away from the internal energy of the subsystem, here the atom, then the rate response is negative $\mathcal{W}^{(\text{Resp})} \leq 0$, and the constraints become trivial, see Appendix G.

In Fig. 4, we also see that the thermodynamic cost and the energetic cost are very similar, and that there is no hierarchy between them, namely it depends on the specific parameters whether the thermodynamic or the energetic cost is larger. This can be seen in panel (b), where, in the absence of Kerr non-linearity the thermodynamic cost is larger than the energetic one, but in the presence of such a non-linearity the opposite holds true.

B. Coupled fermionic rings

Here, we consider two tight-binding fermionic rings with L_α sites for subsystem $\alpha = D, U$. Their Hamil-

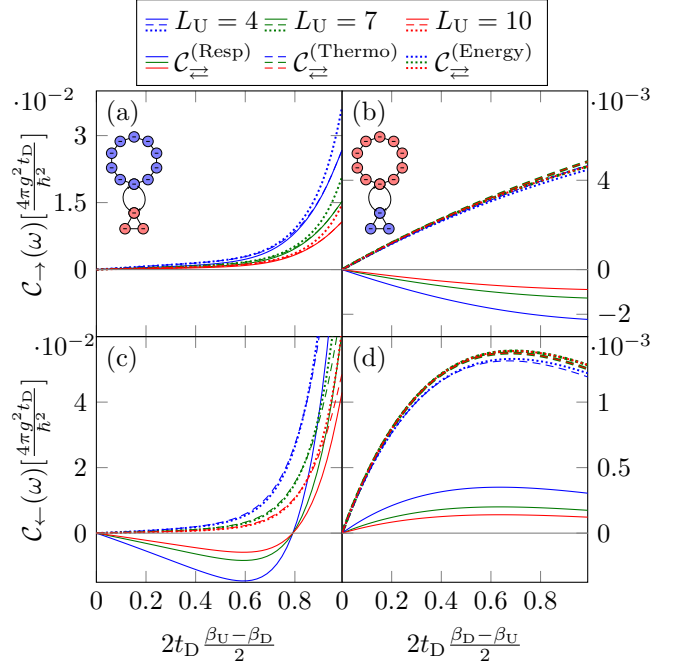


Figure 6. Thermodynamic cost (dashed lines), energetic cost (dotted lines), and rate response (solid lines) for the two coupled fermionic rings with charging energies $u_D/2t_D = 10, u_U = 0$, plotted vs the inverse temperature difference $\beta_U - \beta_D$. The down ring has fixed size $L_L = 3$, and the upper ring has sizes $L_U = 4, 7, 10$ for the curves in blue, green, and red, respectively. All other parameters are the same as in Fig. 5. In panels (a, c), the upper, larger ring is kept at the cold temperature ($\beta_U > \beta_D$), whereas in panels (b, d) the down, smaller ring is kept fixed at the cold temperature ($\beta_D > \beta_U$).

tonians read

$$\hat{H}_\alpha = \sum_{i=0}^{L_\alpha-1} t_\alpha (\hat{c}_{\alpha,i+1}^\dagger \hat{c}_{\alpha,i} + \hat{c}_{\alpha,i}^\dagger \hat{c}_{\alpha,i+1}) + \frac{u_\alpha}{2} \hat{N}_\alpha (\hat{N}_\alpha - 1), \quad (26)$$

where we take periodic boundary conditions $\hat{c}_{\alpha,L_\alpha} = \hat{c}_{\alpha,0}$ for the fermionic operators obeying $\{\hat{c}_{\alpha,i}, \hat{c}_{\beta,j}^\dagger\} = \delta_{\alpha\beta}\delta_{ij}$. The charging energy contribution in Eq. (26), parametrized by u_α , depends on $\hat{N}_\alpha = \sum_{i=0}^{L_\alpha-1} \hat{c}_{\alpha,i}^\dagger \hat{c}_{\alpha,i}$, i.e., the total number operator for subsystem α . Next, we introduce weak tunneling between the two rings, taken at the site $i = 0$, by adding the tunneling Hamiltonian

$$\hat{V}(t) = g \left(\hat{c}_{D,0}^\dagger \hat{c}_{U,0} e^{-i\omega t} + \hat{c}_{U,0}^\dagger \hat{c}_{D,0} e^{i\omega t} \right), \quad (27)$$

with $g \ll t$. Here, we identify the tunneling operator $\hat{A} = g \hat{c}_{D,0}^\dagger \hat{c}_{U,0}$, which transfers a fermion from the up ring (U) to the down ring (D). Then, using this tunneling operator \hat{A} , we calculate the amplitudes $\mathcal{C}_{\leftrightarrow}^{(i)}(\omega)$ of Eq. (23). Note that a possible observable \hat{Q} could here be the number of fermions in one ring, e.g. $\hat{Q} = \hat{N}_D$, which

satisfies $[\hat{Q}, \hat{A}] = \hat{A}$. The result for $\mathcal{C}_{\leftrightarrow}^{(i)}(\omega)$ is shown in Fig. 5, where we plot $\mathcal{C}_{\leftrightarrow}^{(i)}(\omega)$ at different values of the charging energy u_D and in Fig. 6 for different sizes L_U . Note that the frequency ω of the tunneling Hamiltonian can emerge from a potential bias between the rings after a gauge transformation [28, 74]. Similarly to the atom-cavity system considered in Sec. IV A, the charging energy u_D produces nontrivial constraints for both Γ_{\leftrightarrow} , as shown in panels (a, c) of Fig. 5, when the down ring is the one that is considered at two different temperatures when comparing out-of-equilibrium rates. By contrast, for vanishing charging energy $u_U = 0$, only the rate Γ_{\leftarrow} is non-trivially constrained, see panels (b, d), for the case where it is the upper ring that is taken at two different temperatures.

Furthermore, as discussed in Sec. III C, increasing the size of the ring that is considered at two different temperatures, when comparing out-of-equilibrium rates, weakens the constraints, as is seen in panels (b, d) of Fig. 6. In this example, the tunneling rates scale inversely with the ring size, i.e. with a scaling function f on the form $f(L_U) \sim 1/L_U$ [see below Eq. (21)], whereas the extensive quantities entering the thermodynamic and energetic costs scale linearly with L_U . Thus, while the costs are essentially unaffected upon increasing L_U , the rate responses instead decrease. By contrast, if the ring that is considered at two different temperatures has a fixed size, both costs and rate responses scale as $1/L_U$ because of the scaling of the tunneling rates alone, see panels (a, c). This feature implies that, as long as the size of the subsystem considered at two different temperatures remains small, there are nontrivial constraints on the tunneling rates, irrespective of the size of the subsystem with fixed temperature.

V. CONCLUSIONS

We have studied the tunneling rates of transitions between two weakly coupled, but otherwise generic, subsystems driven out of equilibrium by a temperature bias. For such setups, we have proved two novel bounds that the resulting out-of-equilibrium tunneling rates (6) satisfy: i) The thermodynamic constraint (16), stating that the out-of-equilibrium response of the tunneling rates bounds from below the magnitude of the rates themselves multiplied by the heat dissipated while establishing or depleting the temperature bias. ii) The energetic constraint (20), which states that the out-of-equilibrium response of the tunneling rates also bounds from below the tunneling rates weighted by the continuous change in the internal energy required to heat one of the subsystems. As a key consequence of these bounds, also the tunneling current and its low-frequency noise become bounded in the presence of a temperature bias.

Our results thus highlight a fundamental connection between thermodynamic potentials and transport quantities for small-size quantum systems. In particular, they

should be testable for a broad range of state-of-the-art experimental setups, including optical or mechanical cavities coupled together [61] or to (artificial) atoms [62–67], and tunneling bridges across molecules [38, 40, 68] or magnetic impurities [69–71].

ACKNOWLEDGMENTS

We gratefully acknowledge funding from the Knut and Alice Wallenberg foundation via the fellowship program (L.T. and J.S.), the European Research Council (ERC) under the European Union’s Horizon Europe research and innovation program (101088169/NanoRecycle) (J.S.), from the Swedish Vetenskapsrådet via Project No. 2023-04043 (C.S.), and from the European Union’s Horizon 2020 research and innovation programme under grant agreement No 101031655 (TEAPOT) (C.S.).

Appendix A: Perturbative expansion of current and noise

In this Appendix, we re-derive the expressions (8) for the current I and the noise S obtained in Refs. [17, 24, 26]. As our starting point, we consider the unitary evolution from time 0 to time t of the full Hamiltonian $\hat{H}(t) = \hat{H}_0 + \hat{V}(t)$. The time evolution operator reads

$$\hat{\mathcal{U}}(t, 0) = \mathcal{T} \exp \left\{ -\frac{i}{\hbar} \int_0^t \hat{H}(s) ds \right\}, \quad (\text{A1})$$

where \mathcal{T} denotes the time ordering. By treating the tunneling Hamiltonian $\hat{V}(t)$ perturbatively, we next expand the full unitary evolution as $\hat{\mathcal{U}}(t, 0) \approx \hat{\mathcal{U}}_0(t, 0) + \delta\hat{\mathcal{U}}(t, 0)$, where

$$\hat{\mathcal{U}}_0(t, 0) \equiv e^{-i\hat{H}_0 t/\hbar}, \quad (\text{A2a})$$

$$\delta\hat{\mathcal{U}}(t, 0) \equiv -\frac{i}{\hbar} \int_0^t dx \hat{\mathcal{U}}_0(t, x) \hat{V}(x) \hat{\mathcal{U}}_0(x, 0), \quad (\text{A2b})$$

are the evolution induced by the free Hamiltonian \hat{H}_0 and the first correction due to the tunneling Hamiltonian $\hat{V}(t)$, respectively.

With Eq. (A2), also the average current can be expanded in powers of the tunneling operator A as $\langle \hat{I}_H(t) \rangle \approx I^{(1)}(t) + I^{(2)}(t)$ with

$$I^{(1)}(t) \equiv \text{Tr} \left\{ \hat{\mathcal{U}}_0^\dagger(t, 0) \hat{I}(t) \hat{\mathcal{U}}_0(t, 0) \hat{\rho}_0 \right\}, \quad (\text{A3a})$$

$$I^{(2)}(t) \equiv \text{Tr} \left\{ [\delta\hat{\mathcal{U}}^\dagger(t, 0) \hat{I}(t) \hat{\mathcal{U}}_0(t, 0) + \hat{\mathcal{U}}_0^\dagger \hat{I}(t) \delta\hat{\mathcal{U}}(t, 0)] \hat{\rho}_0 \right\}, \quad (\text{A3b})$$

with $\hat{I}(t)$ given in Eq. (7). In Eq. (A3), $\hat{\rho}_0$ is the state of the system at time $t = 0$. In the following, we assume that $[\hat{\rho}_0, \hat{H}_0] = 0$, such that, if $\{|a\rangle\}$ are the eigenstates of \hat{H}_0 with energies ϵ_a , their occupations are given by $\hat{\rho}_0 |a\rangle = p_a |a\rangle$.

By defining the matrix elements $A_{ab} \equiv \langle a | \hat{A} | b \rangle$, $A_{ab}^\dagger \equiv \langle a | \hat{A}^\dagger | b \rangle = A_{ba}^*$ and the energy difference $\epsilon_{ba} \equiv \epsilon_b - \epsilon_a$, the first order contribution to the current (A3a) becomes

$$I^{(1)}(t) = -\frac{iq}{\hbar} \sum_a (e^{-i\omega t} A_{aa} - e^{i\omega t} A_{aa}^\dagger) p_a, \quad (\text{A4})$$

and the second order contribution (A3b) becomes

$$\begin{aligned} I^{(2)}(t) &= \frac{q}{\hbar^2} \int_0^t dt' \sum_{ab} p_a \left\{ \left[A_{ab} A_{ba} e^{-i\omega(t'+t)} - \text{c.c.} \right] \times \right. \\ &\quad \times 2i \sin\left[\frac{\epsilon_{ba}}{\hbar}(t-t')\right] + |A_{ba}|^2 2 \cos\left[\left(\frac{\epsilon_{ba}}{\hbar} - \omega\right)(t-t')\right] \\ &\quad \left. - |A_{ab}|^2 2 \cos\left[\left(\frac{\epsilon_{ba}}{\hbar} + \omega\right)(t-t')\right] \right\}. \end{aligned} \quad (\text{A5})$$

Now, since by hypothesis we have $[\hat{Q}, \hat{A}] = q\hat{A}$ and $[\hat{Q}, \hat{H}_0] = 0$, we find that

$$\langle a | [\hat{Q}, \hat{A}] | b \rangle = (q_a - q_b) A_{ab} = q A_{ab}, \quad (\text{A6})$$

where $\hat{Q}|a\rangle = q_a|a\rangle$. This identity implies that $A_{aa} = 0$ (as long as $q \neq 0$), and that $A_{ab} A_{ba} = 0$. Thus, the first order contribution to the current (A4) vanishes, $I^{(1)}(t) = 0$, and the second order contribution (A5) simplifies to

$$\begin{aligned} I^{(2)}(t) &= \frac{q}{\hbar^2} \sum_{ab} p_a \left\{ |A_{ba}|^2 \frac{2 \sin\left[\left(\frac{\epsilon_{ba}}{\hbar} - \omega\right)t\right]}{\frac{\epsilon_{ba}}{\hbar} - \omega} \right. \\ &\quad \left. - |A_{ab}|^2 \frac{2 \sin\left[\left(\frac{\epsilon_{ba}}{\hbar} + \omega\right)t\right]}{\frac{\epsilon_{ba}}{\hbar} + \omega} \right\}, \\ &\stackrel{t \rightarrow \infty}{\rightarrow} \frac{2\pi q}{\hbar^2} \sum_{ab} p_a \left\{ |A_{ba}|^2 \delta\left(\frac{\epsilon_{ba}}{\hbar} - \omega\right) - |A_{ab}|^2 \delta\left(\frac{\epsilon_{ba}}{\hbar} + \omega\right) \right\}, \end{aligned} \quad (\text{A7})$$

which is identical to Eq. (8a).

To calculate the noise we start from the two-time correlator $\mathcal{S}(t) \equiv \langle \hat{I}_H(t) \hat{I}(0) \rangle - \langle \hat{I}_H(t) \rangle \langle \hat{I}(0) \rangle$, which at lowest order in the tunneling operator \hat{A} reads

$$\begin{aligned} \mathcal{S}(t) &\approx \langle \hat{I}_H(t) \hat{I}(0) \rangle \approx \text{Tr} \left\{ \hat{U}_0^\dagger(t, 0) \hat{I}(t) \hat{U}_0(t, 0) \hat{I}(0) \hat{\rho}_0 \right\} \\ &\approx -\frac{q^2}{\hbar^2} \sum_{ab} e^{-i\epsilon_{ba}t/\hbar} p_a \left(e^{-i\omega t} A_{ab} - e^{i\omega t} A_{ab}^\dagger \right) \times \\ &\quad \times \left(A_{ba} - A_{ba}^\dagger \right). \end{aligned} \quad (\text{A8})$$

Similarly to the current, the property Eq. (A6) simplifies this correlator. Then, integrating over time, we obtain the low frequency noise $\mathcal{S} = \int_{-\infty}^{\infty} dt \mathcal{S}(t)$, to lowest order in the tunneling operator \hat{A} as

$$\mathcal{S} \approx \frac{2\pi q}{\hbar^2} \sum_{ab} p_a \left\{ |A_{ba}|^2 \delta\left(\frac{\epsilon_{ba}}{\hbar} - \omega\right) + |A_{ab}|^2 \delta\left(\frac{\epsilon_{ba}}{\hbar} + \omega\right) \right\}. \quad (\text{A9})$$

This expression is equivalent to Eq. (8b).

We finally note that, by exchanging index labels, the current and the noise can we re-written as

$$I \approx \frac{2\pi q}{\hbar^2} \sum_{ab} |A_{ba}|^2 \delta\left(\frac{\epsilon_{ba}}{\hbar} - \omega\right) [p_a - p_b], \quad (\text{A10a})$$

$$S \approx \frac{2\pi q^2}{\hbar^2} \sum_{ab} |A_{ba}|^2 \delta\left(\frac{\epsilon_{ba}}{\hbar} - \omega\right) [p_a + p_b]. \quad (\text{A10b})$$

If the system is initially, at time 0, in equilibrium at the inverse temperature β , the initial state is a Gibbs state $\hat{\rho}_0 \propto e^{-\beta \hat{H}_0}$ and the state occupation probabilities are given as $p_a \propto e^{-\beta \epsilon_a}$. In this case, the products in the summands in Eq. (A10) satisfy

$$\delta\left(\frac{\epsilon_{ba}}{\hbar} - \omega\right) [p_a \pm p_b] = \delta\left(\frac{\epsilon_{ba}}{\hbar} - \omega\right) [e^{-\beta \hbar \omega} \pm 1] p_b, \quad (\text{A11})$$

establishing the equal temperature relation between current and noise, given in Eq. (10).

Appendix B: More general tunneling operators

When more generic tunneling operators are considered, the bounds derived in the main text remain valid for the individual tunneling rates $\Gamma_{\rightleftarrows}$. They do however not extend to the tunneling current and the tunneling current noise.

To show this, in the following, we thus drop the condition $[\hat{Q}, \hat{A}] = q\hat{A}$ on the tunneling operator \hat{A} . Even without this condition, it is possible to define a current operator via Heisenberg's equation of motion as

$$\hat{I}(t) \equiv -\frac{i}{\hbar} \left([\hat{Q}, \hat{A}] e^{-i\omega t} + [\hat{Q}, \hat{A}^\dagger] e^{i\omega t} \right). \quad (\text{B1})$$

Analogously to the derivation in Appendix A, we calculate the lowest-order contributions in the tunneling operator \hat{A} , which now does not satisfy any commutation property with the observable \hat{Q} , but we still assume that it satisfies $A_{ab} A_{ba} = 0$. This constraint means that only one of the transitions between $|a\rangle \rightarrow |b\rangle$ and $|b\rangle \rightarrow |a\rangle$ is possible, where $|a\rangle$ and $|b\rangle$ are the common eigenstates of \hat{H}_0 and \hat{Q} (recall that $[\hat{H}_0, \hat{Q}] = 0$). The forward and the backward rates between these eigenstates are now given as

$$\begin{aligned} \Gamma_{ba}^{\rightarrow} &\equiv \frac{2\pi}{\hbar} \delta(\epsilon_{ba} - \hbar\omega) |A_{ba}|^2 p_a, \\ \Gamma_{ba}^{\leftarrow} &\equiv \frac{2\pi}{\hbar} \delta(\epsilon_{ba} - \hbar\omega) |A_{ba}|^2 p_b. \end{aligned} \quad (\text{B2})$$

With these rates, the current and the noise read

$$\begin{aligned} I &= \sum_{ab} (q_b - q_a) [\Gamma_{ba}^{\rightarrow} - \Gamma_{ba}^{\leftarrow}], \\ \mathcal{S} &= \sum_{ab} (q_b - q_a)^2 [\Gamma_{ba}^{\rightarrow} + \Gamma_{ba}^{\leftarrow}], \end{aligned} \quad (\text{B3})$$

where we recall that $q_a |a\rangle = \hat{Q} |a\rangle$. Specializing to a bipartite system, the rates take the form

$$\begin{aligned}\Gamma_{mk,nl}^{\rightarrow} &\equiv \frac{2\pi}{\hbar} \delta(\epsilon_{mn}^{(\text{L})} + \epsilon_{kl}^{(\text{R})} - \hbar\omega) |A_{mk,nl}|^2 p_n^{(\text{L})} p_l^{(\text{R})}, \\ \Gamma_{mk,nl}^{\leftarrow} &\equiv \frac{2\pi}{\hbar} \delta(\epsilon_{mn}^{(\text{L})} + \epsilon_{kl}^{(\text{R})} - \hbar\omega) |A_{mk,nl}|^2 p_m^{(\text{L})} p_k^{(\text{R})}.\end{aligned}\quad (\text{B4})$$

By inspecting the proofs in Appendix D and F, we find that both the thermodynamic and energetic constraints presented in the main text remain valid for the rates $\Gamma_{mk,nl}^{\leftarrow\rightarrow}$ between each pair of distinct eigenstates. If the hypothesis $[\hat{Q}, \hat{A}] = q\hat{A}$ is restored, one has $(q_{mk} - q_{nl}) \rightarrow q$, and the results in the main text are thus recovered.

Using these rates, the current and noise become

$$\begin{aligned}I &= \sum_{mnkl} (q_{mk} - q_{nl}) [\Gamma_{mk,nl}^{\rightarrow} - \Gamma_{mk,nl}^{\leftarrow}], \\ \mathcal{S} &= \sum_{mnkl} (q_{mk} - q_{nl})^2 [\Gamma_{mk,nl}^{\rightarrow} + \Gamma_{mk,nl}^{\leftarrow}].\end{aligned}\quad (\text{B5})$$

Here, $q_{nl} |nl\rangle = \hat{Q} |nl\rangle$, and the eigenstates $|nl\rangle$ satisfy $\hat{H}_{\text{L}} |nl\rangle = \epsilon_n^{(\text{L})} |nl\rangle$, $\hat{H}_{\text{R}} |nl\rangle = \epsilon_l^{(\text{R})} |nl\rangle$. Therefore, we see that the only difference compared to Eq. (8) in the main text is that the rates at different resonances are weighted with state-dependent factors $(q_{mk} - q_{nl})$ and $(q_{mk} - q_{nl})^2$, instead of the simpler factors q and q^2 . This feature prevents us from defining common global rates with which both the current and the noise can be expressed.

Appendix C: Work extraction and nonequilibrium free energy

By closely following Ref. [75], we show in this Appendix how the nonequilibrium free energy limits work extraction. Consider a system S coupled to a bath B, described by the total Hamiltonian

$$\hat{H}(t) = \hat{H}_{\text{S}}(t) + \hat{H}_{\text{B}} + \hat{H}_{\text{SB}}(t). \quad (\text{C1})$$

Here, $\hat{H}_{\text{S}}(t)$ and \hat{H}_{B} is the system and bath Hamiltonian, respectively, and $\hat{H}_{\text{SB}}(t)$ is the time-dependent coupling between system and bath. The rate of work done on the system and the heat production in the bath are defined as

$$\dot{W}(t) \equiv \text{Tr} \left\{ \frac{d\hat{H}(t)}{dt} \hat{\rho}(t) \right\}, \quad (\text{C2a})$$

$$\begin{aligned}\dot{Q}_{\text{B}}(t) &\equiv \text{Tr} \left\{ \hat{H}_{\text{B}} \frac{d\hat{\rho}(t)}{dt} \right\} \\ &= -\text{Tr} \left\{ \left(\hat{H}_{\text{S}}(t) + \hat{H}_{\text{SB}}(t) \right) \frac{d\hat{\rho}(t)}{dt} \right\},\end{aligned}\quad (\text{C2b})$$

respectively. In this way, we can write an expression equivalent to the first law of thermodynamics. To this

end, one considers the change in the energy of S, denoted $U(t) \equiv \text{Tr} \left\{ (\hat{H}_{\text{S}}(t) + \hat{H}_{\text{SB}}(t)) \hat{\rho}(t) \right\}$, namely

$$\frac{dU(t)}{dt} = \dot{W}(t) - \dot{Q}_{\text{B}}(t). \quad (\text{C3})$$

Integrating from the beginning of the work extraction operation at $t = 0$ to its end at $t = \tau$, we have

$$\Delta U(\tau) \equiv U(\tau) - U(0) = W(\tau) - \Delta Q_{\text{B}}(\tau). \quad (\text{C4})$$

To write an expression equivalent to the second law of thermodynamics, we assume that before the work extraction, the system and the bath are uncorrelated, i.e. $\hat{\rho}(0) = \hat{\rho}_{\text{S}}(0) \otimes \hat{\rho}_{\text{B}}(0)$. Then, the change in entropy of system and bath can be written in terms of the relative entropy between the initial and the time-evolved density matrices. Generally, the relative entropy between two density matrices $\hat{\rho}_1$ and $\hat{\rho}_2$ is defined as

$$D[\hat{\rho}_1 || \hat{\rho}_2] \equiv \text{Tr} \{ \hat{\rho}_1 (\log \hat{\rho}_1 - \log \hat{\rho}_2) \}, \quad (\text{C5})$$

which applied to the evolution of the coupled system and bath becomes

$$D[\hat{\rho}(t) || \hat{\rho}_{\text{S}}(t) \otimes \hat{\rho}_{\text{B}}(t)] = \Delta S_{\text{S}}(t) + \Delta S_{\text{B}}(t) \geq 0. \quad (\text{C6})$$

Here, $\Delta S_{\alpha}(t) \equiv S[\hat{\rho}_{\alpha}(t)] - S[\hat{\rho}_{\alpha}(0)]$ is the difference in von Neumann entropy, and the positivity stems from Klein's inequality. If the bath is sufficiently large, its entropy change is well approximated by the Clausius relation

$$\Delta S_{\text{B}}(t) \approx \frac{\Delta Q_{\text{B}}(t)}{T_{\text{B}}}, \quad (\text{C7})$$

where T_{B} is the temperature of the bath. Then, combining Eqs. (C4, C6, C7) we find that the performed work is limited from below by the nonequilibrium free energy ΔF as

$$W(\tau) \geq \Delta U(\tau) - T_{\text{B}} \Delta S_{\text{S}}(\tau) \equiv \Delta F. \quad (\text{C8})$$

In this work, we are interested in the situation where, at the beginning and at the end of the operation, the system Hamiltonian and the system-bath interaction satisfy

$$\hat{H}_{\text{S}}(0) = \hat{H}_{\text{S}}(\tau), \quad \hat{H}_{\text{SB}}(0) = \hat{H}_{\text{SB}}(\tau) = 0, \quad (\text{C9})$$

i.e. the system's Hamiltonian is left unchanged after the operation, and the system and the bath are not coupled at the beginning and at the end of the operation. Then, the nonequilibrium free energy reads

$$\Delta F = \Delta F_{\text{S}} = \Delta U_{\text{S}}(\tau) - T_{\text{B}} \Delta S_{\text{S}}(\tau) \quad (\text{C10})$$

with $\Delta U_{\text{S}}(\tau) \equiv U_{\text{S}}(\tau) - U_{\text{S}}(0)$ and $U_{\text{S}}(t) \equiv \text{Tr}_{\text{S}} \{ \hat{H}_{\text{S}}(t) \hat{\rho}_{\text{S}}(t) \}$. These features allow us to calculate the maximum work that can be extracted $W^{\text{ext}}(\tau) = -W(\tau)$ by using only the knowledge of the system's density matrix at the beginning and at the end of the operation:

$$W^{\text{ext}}(\tau) \leq -\Delta F_{\text{S}}. \quad (\text{C11})$$

Furthermore, if the initial and final states of the system are thermal states at temperatures T and T_B , respectively, the entropy variation of the system reads

$$\Delta S_S(\tau) = \beta \Delta U_S(\tau) + (\beta_B - \beta) U_S(\tau) + \log \left(\frac{Z_S(\tau)}{Z_S(0)} \right), \quad (\text{C12})$$

with $Z_S(0) = \text{Tr}_S \left\{ \exp(-\beta \hat{H}_S(0)) \right\}$ and $Z_S(\tau) = \text{Tr}_S \left\{ \exp(-\beta_B \hat{H}_S(\tau)) \right\}$ being the partition functions at the inverse temperatures $\beta = T^{-1}$ and $\beta_B = T_B^{-1}$, respectively. We now recall that the internal energy of a thermal state is related to the partition function as $U_S(\tau) = -\frac{\partial}{\partial \beta_B} \log Z_S(\tau)$, and by using the concavity of $-\log Z_S$ as a function of the inverse temperature, Eq. (C12) leads to the inequality

$$\Delta S_S(\tau) \leq \beta \Delta U_S(\tau). \quad (\text{C13})$$

We next combine Eqs. (C4, C6, C13) in two different ways, depending on whether we focus on the heat absorbed by the bath, $\Delta Q_B(\tau)$, or on the energy variation in the system $\Delta U_S(\tau)$. For these two situations, we find

$$W(\tau) - \left(1 - \frac{T_B}{T}\right) \Delta U_S(\tau) \geq 0, \quad (\text{C14a})$$

$$W(\tau) - \left(1 - \frac{T}{T_B}\right) \Delta Q_B(\tau) \geq 0. \quad (\text{C14b})$$

As detailed in Fig. 1, we are interested in both cases $T < T_B$ and $T > T_B$, depending on whether we are cooling or heating subsystem L. When $T < T_B$, we focus on Eq. (C14a). There, $\Delta U_S(\tau) \geq 0$, since the system is heated by the hot bath, and $W(\tau) \leq 0$ since we are using the heat flow to extract energy. Then

$$\Delta U_S(\tau) \geq W^{\text{ext}}(\tau) \frac{T}{T_B - T} = W^{\text{ext}}(\tau) \eta^{(\text{c})}. \quad (\text{C15})$$

Instead, when $T > T_B$, we focus on Eq. (C14b), where $\Delta Q_B(\tau) \geq 0$ as the cold bath receives heat from the (initially hotter) system, and again $W(\tau) \leq 0$ as we are extracting work. Then,

$$\Delta Q_B(\tau) \geq W^{\text{ext}}(\tau) \frac{T_B}{T_B - T} = W^{\text{ext}}(\tau) \eta^{(\text{h})}. \quad (\text{C16})$$

Appendix D: Derivation of the thermodynamic constraint

In this Appendix, we prove Eq. (16) for the forward tunneling rate Γ_{\rightarrow} in Eq. (6). The proof for Γ_{\leftarrow} is analogous. The difference between out-of-equilibrium rates $\Gamma_{\rightarrow}(\beta_{L,1}, \beta_R)$ and $\Gamma_{\rightarrow}(\beta_{L,2}, \beta_R)$ reads

$$\begin{aligned} \Gamma_{\rightarrow}(\beta_{L,1}, \beta_R) - \Gamma_{\rightarrow}(\beta_{L,2}, \beta_R) &= \frac{2\pi}{\hbar} \sum_{nmkl} |\mathcal{A}_{nmkl}|^2 \times \\ &\times \delta(\epsilon_{mn}^{(\text{L})} + \epsilon_{kl}^{(\text{R})} - \hbar\omega) \left[\frac{e^{-\beta_{L,1}\epsilon_n^{(\text{L})}}}{Z_L(\beta_{L,1})} - \frac{e^{-\beta_{L,2}\epsilon_n^{(\text{L})}}}{Z_L(\beta_{L,2})} \right] \frac{e^{-\beta_R\epsilon_l^{(\text{R})}}}{Z_R(\beta_R)}. \end{aligned} \quad (\text{D1})$$

Here, the difference between the occupation probabilities of subsystem L vanishes at the special energy

$$\tilde{\epsilon}^{(\text{L})} = \frac{1}{\beta_{L,1} - \beta_{L,2}} \log \frac{Z_L(\beta_{L,2})}{Z_L(\beta_{L,1})}. \quad (\text{D2})$$

When $\beta_{L,1} \geq \beta_{L,2}$, we then find that the following inequality holds:

$$\begin{aligned} e^{\alpha\epsilon_n^{(\text{L})}} \left(\frac{e^{-\beta_{L,1}\epsilon_n^{(\text{L})}}}{Z_L(\beta_{L,1})} - \frac{e^{-\beta_{L,2}\epsilon_n^{(\text{L})}}}{Z_L(\beta_{L,2})} \right) &\leq \\ &\leq e^{\alpha\tilde{\epsilon}^{(\text{L})}} \left(\frac{e^{-\beta_{L,1}\epsilon_n^{(\text{L})}}}{Z_L(\beta_{L,1})} - \frac{e^{-\beta_{L,2}\epsilon_n^{(\text{L})}}}{Z_L(\beta_{L,2})} \right) \end{aligned} \quad (\text{D3})$$

for any real number $\alpha \geq 0$ and for all $\epsilon_n^{(\text{L})}$. Note that this relation becomes an equality for $\epsilon_n^{(\text{L})} = \tilde{\epsilon}^{(\text{L})}$. Saturating this inequality is necessary to obtain a nontrivial equality in the thermodynamic constraint. Specifically, such a condition is achieved with a tunneling operator \hat{A} allowing transitions starting from states of subsystem L that have this specific energy $\epsilon_n^{(\text{L})} = \tilde{\epsilon}^{(\text{L})}$.

Using this inequality for all resonances in Eq. (D1), we have

$$\begin{aligned} \Gamma_{\rightarrow}(\beta_{L,1}, \beta_R) - \Gamma_{\rightarrow}(\beta_{L,2}, \beta_R) &\leq \frac{2\pi}{\hbar} e^{\alpha\tilde{\epsilon}^{(\text{L})}} \times \\ &\times \sum_{nmkl} |\mathcal{A}_{nmkl}|^2 \delta(\epsilon_{mn}^{(\text{L})} + \epsilon_{kl}^{(\text{R})} - \hbar\omega) \times \\ &\times \left[\frac{e^{-(\beta_{L,1} + \alpha)\epsilon_n^{(\text{L})}}}{Z_L(\beta_{L,1})} - \frac{e^{-(\beta_{L,2} + \alpha)\epsilon_n^{(\text{L})}}}{Z_L(\beta_{L,2})} \right] \frac{e^{-\beta_R\epsilon_l^{(\text{R})}}}{Z_R(\beta_R)}. \end{aligned} \quad (\text{D4})$$

Here, we recognize the occupation probabilities at different temperatures, which allows us to write

$$\begin{aligned} \Gamma_{\rightarrow}(\beta_{L,1}, \beta_R) - \Gamma_{\rightarrow}(\beta_{L,2}, \beta_R) &\leq e^{\alpha\tilde{\epsilon}^{(\text{L})}} \times \\ &\times \left[\frac{Z_L(\beta_{L,1} + \alpha)}{Z_L(\beta_{L,1})} \Gamma_{\rightarrow}(\beta_{L,1} + \alpha, \beta_R) + \right. \\ &\left. - \frac{Z_L(\beta_{L,2} + \alpha)}{Z_L(\beta_{L,2})} \Gamma_{\rightarrow}(\beta_{L,2} + \alpha, \beta_R) \right] \end{aligned} \quad (\text{D5})$$

for all $\alpha \geq 0$ and $\beta_{L,1} > \beta_{L,2}$. To avoid dealing with too many different temperatures, we study how Eq. (D5) behaves as $\alpha/\beta_{L,i/R} \rightarrow 0^+$. In particular, to zeroth order in α , the right-hand side cancels with the left-hand side. The first-order contribution in α leads instead to the inequality

$$\begin{aligned} \tilde{\epsilon}^{(\text{L})} [\Gamma_{\rightarrow}(\beta_{L,1}, \beta_R) - \Gamma_{\rightarrow}(\beta_{L,2}, \beta_R)] &+ \\ &+ [\partial_{\beta} \log Z_L(\beta_{L,1})] \Gamma_{\rightarrow}(\beta_{L,1}, \beta_R) + \\ &- [\partial_{\beta} \log Z_L(\beta_{L,1})] \Gamma_{\rightarrow}(\beta_{L,2}, \beta_R) \geq \\ &\geq \partial_L \Gamma_{\rightarrow}(\beta_{L,2}, \beta_R) - \partial_L \Gamma_{\rightarrow}(\beta_{L,1}, \beta_R), \end{aligned} \quad (\text{D6})$$

where $\partial_L \Gamma_{\rightarrow}(x, y) \equiv \frac{\partial \Gamma_{\rightarrow}}{\partial x}(x, y)$. Here, we already recognize the structure of the rate response on the right-hand side of the inequality. Recalling that $\partial_{\beta} \log Z_L(\beta) =$

$-U_L(\beta)$, we see that the rates are multiplied by the differences

$$\begin{aligned}\tilde{\epsilon}^{(L)} - U_L(\beta_{L,1}) &= \frac{\Delta S_L - \beta_{L,2} \Delta U_L}{\beta_{L,1} - \beta_{L,2}} = -\frac{\beta_{L,2} \Delta F_L^{(h)}}{\beta_{L,1} - \beta_{L,2}}, \\ \tilde{\epsilon}^{(L)} - U_L(\beta_{L,2}) &= \frac{\Delta S_L - \beta_{L,1} \Delta U_L}{\beta_{L,1} - \beta_{L,2}} = \frac{\beta_{L,1} \Delta F_L^{(c)}}{\beta_{L,1} - \beta_{L,2}}\end{aligned}\quad (D7)$$

where $\Delta U_L \equiv U_L(\beta_{L,2}) - U_L(\beta_{L,1})$ and $\Delta S_L \equiv S_L(\beta_{L,2}) - S_L(\beta_{L,1})$. The nonequilibrium free energy variations $\Delta F_L^{(h/c)}$ are defined with respect to the hot (cold) temperature $\beta_{L,2}^{-1}$ ($\beta_{L,1}^{-1}$) as

$$\begin{aligned}\Delta F_L^{(h)} &\equiv \Delta U_L - T_{L,2} \Delta S_L, \\ \Delta F_L^{(c)} &\equiv -\Delta U_L + T_{L,1} \Delta S_L.\end{aligned}\quad (D8)$$

Then, combining Eqs. (D6) and (D7), we find

$$\begin{aligned}-\frac{T_{L,1} \Delta F_L^{(h)}}{T_{L,2} - T_{L,1}} \Gamma_{\rightarrow}(\beta_{L,1}, \beta_R) - \frac{T_{L,2} \Delta F_L^{(c)}}{T_{L,2} - T_{L,1}} \Gamma_{\rightarrow}(\beta_{L,2}, \beta_R) &\geq \\ \geq \partial_L \Gamma_{\rightarrow}(\beta_{L,2}, \beta_R) - \partial_L \Gamma_{\rightarrow}(\beta_{L,1}, \beta_R),\end{aligned}\quad (D9)$$

which holds for $\beta_{L,1} > \beta_{L,2}$. By choosing $\beta_{L,1} = \beta_R$ and any hotter inverse temperature as $\beta_{L,2} = \beta_L$, we arrive at Eq. (16).

Notably, the derivatives in the rate response $\mathcal{W}_{\rightleftarrows}^{(\text{Resp})}$ [Eq. (17)] can alternatively be understood in terms of higher-order correlation functions of the tunneling operator \hat{A} in (5). More specifically, we find that

$$\begin{aligned}\frac{\partial \Gamma_{\rightarrow}}{\partial \beta_L} &= \frac{1}{\hbar^2} \int dt \langle \hat{A}_H^\dagger(t) e^{i\omega t} \hat{A} [U_L - \hat{H}_L] \rangle, \\ \frac{\partial \Gamma_{\leftarrow}}{\partial \beta_L} &= \frac{1}{\hbar^2} \int dt \langle \hat{A}_H(t) e^{-i\omega t} \hat{A}^\dagger [U_L - \hat{H}_L] \rangle,\end{aligned}\quad (D10)$$

where we recall that $\hat{A}_H(0) = \hat{A}$.

Appendix E: Grönwall inequality on out-of-equilibrium rates

From the thermodynamic constraint in Eq. (16), it is possible to remove the out-of-equilibrium response of tunneling rates, $\frac{\partial \Gamma_{\rightleftarrows}}{\partial \beta_L}(\beta_L, \beta_R)$, by means of Grönwall's lemma [76]. Indeed, Eq. (16) can be cast as

$$y'(x) \leq f(x) + g(x)y(x), \quad (E1)$$

where x is the inverse temperature of subsystem L, and

$$\begin{aligned}y(x) &\equiv \Gamma_{\rightleftarrows}(x, \beta_R), \\ f(x) &\equiv \frac{\partial \Gamma_{\rightleftarrows}}{\partial \beta_L}(\beta_R, \beta_R) - \Delta F_L^{(c)}(x) \eta^{(h)}(x) \Gamma_{\rightleftarrows}(\beta_R, \beta_R), \\ g(x) &\equiv -\Delta F_L^{(h)}(x) \eta^{(c)}(x).\end{aligned}\quad (E2)$$

Considering the corresponding homogeneous differential equation,

$$v'(x) = g(x)v(x) \quad \rightarrow \quad v(x) = \exp \left[\int_x^{\beta_R} g(s) ds \right], \quad (E3)$$

we see that $v(\beta_R) = 1$ and $v(x) \geq 0$ for all x . The derivative of $y(x)/v(x)$ reads

$$\frac{d}{dx} \frac{y(x)}{v(x)} = \frac{v(x)y'(x) - y(x)v'(x)}{v(x)^2} \leq \frac{f(x)}{v(x)}. \quad (E4)$$

Integrating this expression from β_L to β_R leads to

$$y(\beta_R) - \frac{y(\beta_L)}{v(\beta_L)} \leq \int_{\beta_R}^{\beta_L} f(x) \exp \left[- \int_x^{\beta_R} g(s) ds \right] dx, \quad (E5)$$

which is Grönwall's inequality. Reordering the terms we find

$$\begin{aligned}\Gamma_{\rightleftarrows}(\beta_L, \beta_R) &\geq \Gamma_{\rightleftarrows}(\beta_R, \beta_R) \exp \left[\int_{\beta_L}^{\beta_R} g(x) dx \right] + \\ &- \int_{\beta_L}^{\beta_R} f(x) \exp \left[\int_{\beta_L}^x g(s) ds \right] dx.\end{aligned}\quad (E6)$$

Notably, the right-hand side of Eq. (E6) contains neither the out-of-equilibrium rates nor their derivatives.

Appendix F: Derivation of the energetic constraint

In this Appendix, we prove the energetic constraint in Eq. (20) in differential form, namely

$$\frac{\partial^2 \Gamma_{\rightleftarrows}}{\partial \beta_L^2}(\beta_L, \beta_R) \geq \frac{\partial U_L}{\partial \beta_L}(\beta_L) \Gamma_{\rightleftarrows}(\beta_L, \beta_R). \quad (F1)$$

By integrating over β_L from an initial inverse temperature $\beta_{L,1}$ to a final one $\beta_{L,2}$, one can then reach the integral form in Eq. (20). As in Appendix D, here we prove the energetic constraint only for Γ_{\rightarrow} since the proof for Γ_{\leftarrow} is analogous. First, notice that the β_L -derivatives act only on the occupation probabilities of subsystem L,

$$\frac{\partial^2 \Gamma_{\rightarrow}}{\partial \beta_L^2} = \frac{4\pi}{\hbar} \sum_{nmlk} |\mathcal{A}_{nmlk}|^2 \delta(\epsilon_{mn}^{(L)} + \epsilon_{kl}^{(R)} - \hbar\omega) \frac{\partial^2 p_n^{(L)}}{\partial \beta_L^2} p_l^{(R)}. \quad (F2)$$

Then, recalling that the internal energy satisfies $U_L(\beta_L) = -\frac{\partial \log Z_L(\beta_L)}{\partial \beta_L}$, the derivative of the occupation probabilities reads

$$\begin{aligned}\frac{\partial^2 p_n^{(L)}}{\partial \beta_L^2} &= \frac{\partial}{\partial \beta_L} \left[\left(-\epsilon_n^{(L)} + U_L(\beta_L) \right) p_n^{(L)} \right] \\ &= \left[\frac{\partial U_L(\beta_L)}{\partial \beta_L} + \left(U_L(\beta_L) - \epsilon_n^{(L)} \right)^2 \right] p_n^{(L)} \\ &\geq \frac{\partial U_L(\beta_L)}{\partial \beta_L} p_n^{(L)}.\end{aligned}\quad (F3)$$

Substituting this inequality in Eq. (F2) we find Eq. (F1). Furthermore, we see here that the inequality is saturated when $|\mathcal{A}_{nmlk}|^2 \delta(\epsilon_{mn}^{(L)} + \epsilon_{kl}^{(R)} - \hbar\omega)$ is nonzero only for energies $\epsilon_n^{(L)}$ close to the internal energy $U_L(\beta_L)$.

Appendix G: Sufficient condition for trivial constraints

Both thermodynamic and energetic cost, Eqs. (15) and (20) respectively, are positive by definition, and are lower-bounded by the rate response $\mathcal{W}^{(\text{Resp})}$ in Eq. (17). Therefore, the thermodynamic and energetic constraints are nontrivial whenever $\mathcal{W}_{\rightleftarrows}^{(\text{Resp})} > 0$. In this appendix we provide sufficient conditions for $\mathcal{W}_{\rightleftarrows}^{(\text{Resp})} \leq 0$, making the results of Eqs. (16, 20) trivial. Like the previous appendices, we provide the derivation for the forward process. Starting from the definition of the rate response, the derivatives with respect to β_L act only on the probabilities $p_n^{(L)}$. Specifically, the rate response becomes

$$\mathcal{W}_{\rightleftarrows}^{(\text{Resp})} = \frac{2\pi}{\hbar} \sum_{nmlk} |\mathcal{A}_{nmlk}|^2 \delta(\epsilon_{mn}^{(L)} + \epsilon_{kl}^{(R)} - \hbar\omega) \times \times \left[\partial_L p_n^{(L)}(\beta_{L,2}) - \partial_L p_n^{(L)}(\beta_{L,1}) \right] p_l^{(R)}(\beta_R) \quad (\text{G1})$$

where the derivative of the probability $p_n^{(L)}$ reads

$$\partial_L p_n^{(L)}(\beta) = \left[U_L(\beta) - \epsilon_n^{(L)} \right] p_n^{(L)}(\beta). \quad (\text{G2})$$

Taking a second derivative with respect to β we find

$$\partial_L^2 p_n^{(L)}(\beta) = \left[\partial_L U_L(\beta) + [U_L(\beta) - \epsilon_n^{(L)}]^2 \right] p_n^{(L)}(\beta). \quad (\text{G3})$$

We now focus on all energies $\epsilon_n^{(L)}$ lying far away from the internal energy U_L . Namely, we suppose that the

following inequality holds for all $\beta \in [\beta_{L,2}, \beta_{L,1}]$,

$$|U_L(\beta) - \epsilon_n^{(L)}| \geq \sqrt{-\partial_L U_L(\beta)} = \delta U_L(\beta), \quad (\text{G4})$$

where $\delta U_L(\beta) = \sqrt{\sum_n (\epsilon_n^{(L)})^2 p_n^{(L)}(\beta) - U_L^2(\beta)}$ is the standard deviation of the internal energy. In this energy interval, the second derivative of the occupation probabilities is positive, i.e. $\partial_L^2 p_n^{(L)}(\beta) \geq 0$, making $\partial_L p_n^{(L)}(\beta)$ an increasing function in the inverse temperature β . This in turn makes the rate response negative,

$$\partial_L p_n^{(L)}(\beta_{L,1}) - \partial_L p_n^{(L)}(\beta_{L,2}) \geq 0 \Rightarrow \mathcal{W}_{\rightleftarrows}^{(\text{Resp})} \leq 0, \quad (\text{G5})$$

thus trivializing both thermodynamic and energetic constraint.

Conversely, the initial states' energies lying *within* a standard deviation from the internal energy for all inverse temperatures in $[\beta_{L,2}, \beta_{L,1}]$ is a sufficient condition for the rate response to be positive $\mathcal{W}_{\rightleftarrows}^{(\text{Resp})} \geq 0$. Indeed, this condition on the energies makes $\partial_L p_n^{(L)}(\beta)$ a decreasing function in the inverse temperature β , leading to

$$\partial_L p_n^{(L)}(\beta_{L,1}) - \partial_L p_n^{(L)}(\beta_{L,2}) \leq 0 \Rightarrow \mathcal{W}_{\rightleftarrows}^{(\text{Resp})} \geq 0. \quad (\text{G6})$$

Specifically, for the two level system considered in Sec. IV A, we can easily compute both the internal energy and its standard deviation

$$U_a(\beta) = \hbar\omega_a p_1^{(a)} \quad (\text{G7})$$

$$\delta U_a(\beta) = \hbar\omega_a \sqrt{p_1^{(a)} [1 - p_1^{(a)}]}$$

with $p_1^{(a)} = (1 + e^{\beta\hbar\omega_a})^{-1} \leq 1/2$. Therefore, when only the transition in which the atom *emits* a photon into the cavity is allowed, the only possible initial state for the atom is the excited one, with energy $\hbar\omega_a$, which however satisfies

$$\hbar\omega_a \geq U_a(\beta) + \delta U_a(\beta) \quad (\text{G8})$$

for all β . Therefore, the rate response associated with the emission of a photon is always negative, and it does neither put a constraint on the thermodynamic cost nor on the energetic cost.

[1] C. Jarzynski, Nonequilibrium Equality for Free Energy Differences, *Phys. Rev. Lett.* **78**, 2690 (1997).

[2] G. E. Crooks, Entropy production fluctuation theorem and the nonequilibrium work relation for free energy differences, *Phys. Rev. E* **60**, 2721 (1999).

[3] H. Tasaki, Jarzynski Relations for Quantum Systems and Some Applications, arXiv 10.48550/arXiv.cond-mat/0009244 (2000), *cond-mat/0009244*.

[4] D. Andrieux and P. Gaspard, A fluctuation theorem for currents and non-linear response coefficients, *J. Stat. Mech.: Theory Exp.* **2007** (02), P02006.

[5] C. Jarzynski, Comparison of far-from-equilibrium work relations, *C. R. Phys.* **8**, 495 (2007).

[6] D. Andrieux, P. Gaspard, T. Monnai, and S. Tasaki, The fluctuation theorem for currents in open quantum systems, *New J. Phys.* **11**, 043014 (2009).

[7] M. Esposito, U. Harbola, and S. Mukamel, Nonequilibrium fluctuations, fluctuation theorems, and counting statistics in quantum systems, *Rev. Mod. Phys.* **81**, 1665 (2009).

[8] T. Sagawa and M. Ueda, Nonequilibrium thermodynamics of feedback control, *Phys. Rev. E* **85**, 021104 (2012).

[9] O.-P. Saira, Y. Yoon, T. Tanttu, M. Möttönen, D. V. Averin, and J. P. Pekola, Test of the Jarzynski and Crooks Fluctuation Relations in an Electronic System, *Phys. Rev. Lett.* **109**, 180601 (2012).

[10] G. N. Bochkov and Y. E. Kuzovlev, Fluctuation–dissipation relations. Achievements and misunderstandings, *Phys.-Usp.* **56**, 590 (2013).

[11] A. C. Barato and U. Seifert, Thermodynamic Uncertainty Relation for Biomolecular Processes, *Phys. Rev. Lett.* **114**, 158101 (2015).

[12] P. P. Potts and P. Samuelsson, Detailed Fluctuation Relation for Arbitrary Measurement and Feedback Schemes, *Phys. Rev. Lett.* **121**, 210603 (2018).

[13] A. M. Timpanaro, G. Guarneri, J. Goold, and G. T. Landi, Thermodynamic Uncertainty Relations from Exchange Fluctuation Theorems, *Phys. Rev. Lett.* **123**, 090604 (2019).

[14] J. P. Pekola and B. Karimi, Colloquium: Quantum heat transport in condensed matter systems, *Rev. Mod. Phys.* **93**, 041001 (2021).

[15] P. Strasberg, *Quantum Stochastic Thermodynamics* (Oxford University Press, Oxford, England, UK, 2022).

[16] G. Guarneri, J. Eisert, and H. J. D. Miller, Generalised linear response theory for the full quantum work statistics, arXiv [10.48550/arXiv.2307.01885](https://arxiv.org/abs/10.48550/arXiv.2307.01885) (2023), [2307.01885](https://arxiv.org/abs/2307.01885).

[17] H. B. Callen and T. A. Welton, Irreversibility and Generalized Noise, *Phys. Rev.* **83**, 34 (1951).

[18] M. S. Green, Markoff Random Processes and the Statistical Mechanics of Time-Dependent Phenomena. II. Irreversible Processes in Fluids, *J. Chem. Phys.* **22**, 398 (1954).

[19] R. Kubo, Statistical-Mechanical Theory of Irreversible Processes. I. General Theory and Simple Applications to Magnetic and Conduction Problems, *J. Phys. Soc. Jpn.* **12**, 570 (1957).

[20] B. Altaner, M. Polettini, and M. Esposito, Fluctuation–Dissipation Relations Far from Equilibrium, *Phys. Rev. Lett.* **117**, 180601 (2016).

[21] A. Dechant and S.-i. Sasa, Fluctuation–response inequality out of equilibrium, *Proc. Natl. Acad. Sci. U.S.A.* **117**, 6430 (2020).

[22] N. Shiraishi, Time-Symmetric Current and Its Fluctuation Response Relation around Nonequilibrium Stalling Stationary State, *Phys. Rev. Lett.* **129**, 020602 (2022).

[23] I. Safi and P. Joyez, Time-dependent theory of nonlinear response and current fluctuations, *Phys. Rev. B* **84**, 205129 (2011).

[24] I. Safi, Time-dependent Transport in arbitrary extended driven tunnel junctions, arXiv [10.48550/arXiv.1401.5950](https://arxiv.org/abs/10.48550/arXiv.1401.5950) (2014), [1401.5950](https://arxiv.org/abs/1401.5950).

[25] I. Safi, Driven quantum circuits and conductors: A unifying perturbative approach, *Phys. Rev. B* **99**, 045101 (2019).

[26] I. Safi, Fluctuation-dissipation relations for strongly correlated out-of-equilibrium circuits, *Phys. Rev. B* **102**, 041113 (2020).

[27] I. Safi, Driven strongly correlated quantum circuits and hall edge states: Unified photoassisted noise and revisited minimal excitations, *Phys. Rev. B* **106**, 205130 (2022).

[28] D. Rogovin and D. J. Scalapino, Fluctuation phenomena in tunnel junctions, *Ann. Phys.* **86**, 1 (1974).

[29] L. S. Levitov and M. Reznikov, Counting statistics of tunneling current, *Phys. Rev. B* **70**, 115305 (2004).

[30] G. Benenti, G. Casati, K. Saito, and R. S. Whitney, Fundamental aspects of steady-state conversion of heat to work at the nanoscale, *Phys. Rep.* **694**, 1 (2017).

[31] R. S. Whitney, R. Sánchez, and J. Splettstoesser, Quantum Thermodynamics of Nanoscale Thermoelectrics and Electronic Devices, in *Thermodynamics in the Quantum Regime* (Springer, Cham, Switzerland, 2019) pp. 175–206.

[32] L. M. Cangemi, C. Bhadra, and A. Levy, Quantum engines and refrigerators, *Phys. Rep.* **1087**, 1 (2024).

[33] H. Thierschmann, R. Sánchez, B. Sothmann, F. Arnold, C. Heyn, W. Hansen, H. Buhmann, and L. W. Molenkamp, Three-terminal energy harvester with coupled quantum dots, *Nat. Nanotechnol.* **10**, 854 (2015).

[34] M. Josefsson, A. Svilans, A. M. Burke, E. A. Hoffmann, S. Fahlvik, C. Thelander, M. Leijnse, and H. Linke, A quantum-dot heat engine operating close to the thermodynamic efficiency limits, *Nat. Nanotechnol.* **13**, 920 (2018).

[35] D. Prete, P. A. Erdman, V. Demontis, V. Zannier, D. Ercole, L. Sorba, F. Beltram, F. Rossella, F. Taddei, and S. Roddaro, Thermoelectric Conversion at 30 K in InAs/InP Nanowire Quantum Dots, *Nano Lett.* **19**, 3033 (2019).

[36] A. Guthrie, C. D. Satrya, Y.-C. Chang, P. Menczel, F. Nori, and J. P. Pekola, Cooper-Pair Box Coupled to Two Resonators: An Architecture for a Quantum Refrigerator, *Phys. Rev. Appl.* **17**, 064022 (2022).

[37] H. Duprez, F. Pierre, E. Sivre, A. Aassime, F. D. Parmentier, A. Cavanna, A. Ouerghi, U. Gennser, I. Safi, C. Mora, and A. Anthore, Dynamical coulomb blockade under a temperature bias, *Phys. Rev. Research* **3**, 023122 (2021).

[38] P. Gehring, J. K. Sowa, C. Hsu, J. de Bruijckere, M. van der Star, J. J. Le Roy, L. Bogani, E. M. Gauger, and H. S. J. van der Zant, Complete mapping of the thermoelectric properties of a single molecule, *Nat. Nanotechnol.* **16**, 426 (2021).

[39] T. Esat, X. Yang, F. Mustafayev, H. Soltner, F. S. Tautz, and R. Temirov, Determining the temperature of a millikelvin scanning tunnelling microscope junction, *Commun. Phys.* **6**, 1 (2023).

[40] A. Gemma, F. Tabatabaei, U. Drechsler, A. Zulji, H. Dekkiche, N. Mosso, T. Niehaus, M. R. Bryce, S. Merabia, and B. Gotsmann, Full thermoelectric characterization of a single molecule, *Nat. Commun.* **14**, 1 (2023).

[41] F. Giazotto, T. T. Heikkilä, A. Luukanen, A. M. Savin, and J. P. Pekola, Opportunities for mesoscopics in thermometry and refrigeration: Physics and applications, *Rev. Mod. Phys.* **78**, 217 (2006).

[42] M. Aspelmeyer, T. J. Kippenberg, and F. Marquardt, Cavity optomechanics, *Rev. Mod. Phys.* **86**, 1391 (2014).

[43] J. Senior, A. Gubaydullin, B. Karimi, J. T. Peltonen, J. Ankerhold, and J. P. Pekola, Heat rectification via a superconducting artificial atom, *Commun. Phys.* **3**, 1 (2020).

[44] E. V. Sukhorukov and D. Loss, Noise in multiterminal diffusive conductors: Universality, nonlocality, and exchange effects, *Phys. Rev. B* **59**, 13054 (1999).

[45] O. S. Lumbroso, L. Simine, A. Nitzan, D. Segal, and O. Tal, Electronic noise due to temperature differences in atomic-scale junctions, *Nature* **562**, 240 (2018).

[46] E. Sivre, H. Duprez, A. Anthore, A. Aassime, F. D. Parmentier, A. Cavanna, A. Ouerghi, U. Gennser, and

F. Pierre, Electronic heat flow and thermal shot noise in quantum circuits, *Nat. Commun.* **10**, 1 (2019).

[47] S. Larocque, E. Pinsolle, C. Lupien, and B. Reulet, Shot Noise of a Temperature-Biased Tunnel Junction, *Phys. Rev. Lett.* **125**, 106801 (2020).

[48] R. A. Melcer, B. Dutta, C. Spånslått, J. Park, A. D. Mirlin, and V. Umansky, Absent thermal equilibration on fractional quantum Hall edges over macroscopic scale, *Nat. Commun.* **13**, 1 (2022).

[49] J. Rech, T. Jonckheere, B. Grémaud, and T. Martin, Negative Delta- T Noise in the Fractional Quantum Hall Effect, *Phys. Rev. Lett.* **125**, 086801 (2020).

[50] M. Hasegawa and K. Saito, Delta- T noise in the Kondo regime, *Phys. Rev. B* **103**, 045409 (2021).

[51] J. Eriksson, M. Acciai, L. Tesser, and J. Splettstoesser, General Bounds on Electronic Shot Noise in the Absence of Currents, *Phys. Rev. Lett.* **127**, 136801 (2021).

[52] G. Zhang, I. V. Gornyi, and C. Spånslått, Delta- T noise for weak tunneling in one-dimensional systems: Interactions versus quantum statistics, *Phys. Rev. B* **105**, 195423 (2022).

[53] A. Popoff, J. Rech, T. Jonckheere, L. Raymond, B. Grémaud, S. Malherbe, and T. Martin, Scattering theory of non-equilibrium noise and delta T current fluctuations through a quantum dot, *J. Phys.: Condens. Matter* **34**, 185301 (2022).

[54] M. Hübner and W. Belzig, Light emission in delta- T -driven mesoscopic conductors, *Phys. Rev. B* **107**, 155405 (2023).

[55] A. Crépieux, T. Q. Duong, and M. Lavagna, Fano factor, ΔT -noise and cross-correlations in double quantum dots, arXiv 10.48550/arXiv.2306.02146 (2023), 2306.02146.

[56] M. Acciai, G. Zhang, and C. Spånslått, Role of scaling dimensions in generalized noises in fractional quantum Hall tunneling due to a temperature bias, arXiv 10.48550/arXiv.2408.04525 (2024), 2408.04525.

[57] L. Tesser and J. Splettstoesser, Out-of-Equilibrium Fluctuation-Dissipation Bounds, *Phys. Rev. Lett.* **132**, 186304 (2024).

[58] J. B. Johnson, Thermal Agitation of Electricity in Conductors, *Nature* **119**, 50 (1927).

[59] H. Nyquist, Thermal Agitation of Electric Charge in Conductors, *Phys. Rev.* **32**, 110 (1928).

[60] Note that it is *not* needed to know the Hamiltonian of the subsystem kept at fixed temperature, which may be arbitrarily complicated, to test these constraints.

[61] R. Leijssen, G. R. La Gala, L. Freisem, J. T. Muhonen, and E. Verhagen, Nonlinear cavity optomechanics with nanomechanical thermal fluctuations, *Nat. Commun.* **8**, 1 (2017).

[62] D. Leibfried, R. Blatt, C. Monroe, and D. Wineland, Quantum dynamics of single trapped ions, *Rev. Mod. Phys.* **75**, 281 (2003).

[63] A. M. Kaufman, B. J. Lester, and C. A. Regal, Cooling a Single Atom in an Optical Tweezer to Its Quantum Ground State, *Phys. Rev. X* **2**, 041014 (2012).

[64] F. Valmorra, K. Yoshida, L. C. Contamin, S. Messelot, S. Massabeau, M. R. Delbecq, M. C. Dartailh, M. M. Desjardins, T. Cubaynes, Z. Leghtas, K. Hirakawa, J. Tignon, S. Dhillon, S. Balibar, J. Mangeney, A. Cottet, and T. Kontos, Vacuum-field-induced THz transport gap in a carbon nanotube quantum dot, *Nat. Commun.* **12**, 1 (2021).

[65] F. Vigneau, J. Monsel, J. Tabanera, K. Aggarwal, L. Bresque, F. Fedele, F. Cerisola, G. A. D. Briggs, J. Anders, J. M. R. Parrondo, A. Auffèves, and N. Ares, Ultra-strong coupling between electron tunneling and mechanical motion, *Phys. Rev. Res.* **4**, 043168 (2022).

[66] S. Haldar, D. Zenelaj, P. P. Potts, H. Havar, S. Lehmann, K. A. Dick, P. Samuelsson, and V. F. Maisi, Microwave power harvesting using resonator-coupled double quantum dot photodiode, *Phys. Rev. B* **109**, L081403 (2024).

[67] S. Sundelin, M. A. Aamir, V. M. Kulkarni, C. Castillo-Moreno, and S. Gasparinetti, Quantum refrigeration powered by noise in a superconducting circuit, arXiv 10.48550/arXiv.2403.03373 (2024), 2403.03373.

[68] E. Pyurbeevea, C. Hsu, D. Vogel, C. Wegeberg, M. Mayor, H. van der Zant, J. A. Mol, and P. Gehring, Controlling the Entropy of a Single-Molecule Junction, *Nano Lett.* **21**, 9715 (2021).

[69] C. Hsu, T. A. Costi, D. Vogel, C. Wegeberg, M. Mayor, H. S. J. van der Zant, and P. Gehring, Magnetic-Field Universality of the Kondo Effect Revealed by Thermocurrent Spectroscopy, *Phys. Rev. Lett.* **128**, 147701 (2022).

[70] U. Thupakula, V. Perrin, A. Palacio-Morales, L. Cario, M. Aprili, P. Simon, and F. Massee, Coherent and Incoherent Tunneling into Yu-Shiba-Rusinov States Revealed by Atomic Scale Shot-Noise Spectroscopy, *Phys. Rev. Lett.* **128**, 247001 (2022).

[71] S. Trishin, C. Lotze, N. Krane, and K. J. Franke, Electronic and magnetic properties of single chalcogen vacancies in MoS₂/Au(111), *Phys. Rev. B* **108**, 165414 (2023).

[72] M. J. Werner and H. Risken, Quasiprobability distributions for the cavity-damped Jaynes-Cummings model with an additional Kerr medium, *Phys. Rev. A* **44**, 4623 (1991).

[73] E. T. Jaynes and F. W. Cummings, Comparison of quantum and semiclassical radiation theories with application to the beam maser, *Proc. IEEE* **51**, 89 (1963).

[74] I. Safi and E. V. Sukhorukov, Determination of tunneling charge via current measurements, *Eur. Phys. Lett.* **91**, 67008 (2010).

[75] M. Esposito, K. Lindenberg, and C. Van den Broeck, Entropy production as correlation between system and reservoir, *New J. Phys.* **12**, 013013 (2010).

[76] T. H. Gronwall, Note on the derivatives with respect to a parameter of the solutions of a system of differential equations, *Annals of Mathematics* **20**, 292 (1919).